RECEIVER DESIGN AND PERFORMANCE ANALYSIS FOR CODE-MULTIPLEXED TRANSMITTED-REFERENCE ULTRA-WIDEBAND SYSTEMS

A THESIS

SUBMITTED TO THE DEPARTMENT OF ELECTRICAL AND

ELECTRONICS ENGINEERING

AND THE INSTITUTE OF ENGINEERING AND SCIENCES

OF BILKENT UNIVERSITY

IN PARTIAL FULFILLMENT OF THE REQUIREMENTS

FOR THE DEGREE OF

MASTER OF SCIENCE

By

Mehmet Emin Tutay

August 2010

I certify that I have read this thesis and that in my opinion it is fully adequate, in scope and in quality, as a thesis for the degree of Master of Science.

_____

Asst. Prof. Dr. Sinan Gezici (Supervisor)

I certify that I have read this thesis and that in my opinion it is fully adequate, in scope and in quality, as a thesis for the degree of Master of Science.

_____

Prof. Dr. Orhan Arıkan

I certify that I have read this thesis and that in my opinion it is fully adequate, in scope and in quality, as a thesis for the degree of Master of Science.

_____

Asst. Prof. Dr. İbrahim Körpeoğlu

Approved for the Institute of Engineering and Sciences:

_____

Prof. Dr. Levent Onural
Director of Institute of Engineering and Sciences

ABSTRACT

RECEIVER DESIGN AND PERFORMANCE ANALYSIS FOR CODE-MULTIPLEXED TRANSMITTED-REFERENCE ULTRA-WIDEBAND SYSTEMS

Mehmet Emin Tutay

M.S. in Electrical and Electronics Engineering

Supervisor: Asst. Prof. Dr. Sinan Gezici

August 2010

In transmitted-reference (TR) and frequency-shifted reference (FSR) ultra-wideband (UWB) systems, data and reference signals are shifted relative to each other in time and frequency domains, respectively. The main advantage of these systems is that they remove strict requirements of channel estimation. In order to implement TR UWB systems, an analog delay line, which is difficult to build in an integrated fashion, is needed. Although FSR systems require frequency conversion at the receiver, which is much simpler in practice, they have data rate limitations. Instead, a code-multiplexed transmitted-reference (CM-TR) UWB system that transmits data and reference signals using two distinct orthogonal codes can be considered. This system requires a simpler receiver and has better performance than TR and FSR.

In the first part of the thesis, CM-TR systems are investigated and probability of error expressions are obtained. For the single user case, a closed-form expression for the exact probability of error is derived. For the multiuser case, a closed-form expression is derived based on the Gaussian approximation, and the

results are compared in different scenarios. In the second part of the thesis, some optimal and suboptimal receivers are studied. First, low complexity receivers, such as the blinking receiver (BR) and the chip discriminator, are presented. The requirements for these types of receivers are explained, and the conditions under which their performance can be improved are discussed. Then, an analytical analysis of the linear minimum mean-squared error (MMSE) receiver and the requirements to implement this MMSE receiver are provided. Lastly, the optimal maximum-likelihood (ML) detector is derived, which has higher computational complexity and more strict requirements than the other receivers. Finally, simulation results are presented in order to verify the theoretical results and to compare the performance of the receivers.

ÖZET

KOD ÇOĞULLAMALI VE REFERANS İLETİMLİ ÇOK GENİŞ BANTLI SİSTEMLER İÇİN ALICI TASARIMI VE PERFORMANS ANALİZİ

Mehmet Emin Tutay
Elektrik ve Elektronik Mühendisliği Bölümü Yüksek Lisans
Tez Yöneticisi: Asst. Prof. Dr. Sinan Gezici
Ağustos 2010

Referans iletimli ve frekans kaydırmalı çok geniş bantlı sistemlerde veri ve referans işaretleri birbirlerine göre zaman ve frekans bölgelerinde kaymış biçimdedir. Bu sistemlerin en büyük avantajı, kanal tahmini ile ilgili zorlu isterlerin kaldırılmasıdır. Referans iletimli çok geniş bantlı sistemlerde, tümdevrelerde kullanılması zor olan analog gecikme hattına ihtiyaç duyulmaktadır. Frekans kaydırmalı referans sistem alıcılarında ise pratikte çok daha basit olan frekans çevrimi işlemi gerekmesine rağmen, bu sistemlerde veri hızı ile ilgili sınırlamalar bulunmaktadır. Bunun yerine, veri ve referans işaretlerini iki ayrı dikgen kod kullanarak ileten, kod çoğullamalı referans iletimli çok geniş bantlı sistem düşünülebilir. Bu sistem, daha basit bir alıcı gerektirmekte ve referans iletimli ve frekans kaydırmalı sistemlere göre daha iyi performans sağlamaktadır.

Tezin ilk kısmında kod çoğullamalı referans iletimli çok geniş bantlı sistemler incelenmekte ve hata olasılığı ifadeleri elde edilmektedir. Tek kullanıcılı durumda, hata olasılığının tam olarak hesaplanmasını sağlayan bir ifade çıkarılmaktadır. Çok kullanıcılı durumda ise, Gauss yaklaşımı temelli bir ifade

elde edilmekte ve sonuçlar farklı senaryolar için kıyaslanmaktadır. Tezin ikinci kısmında, optimal olan ve olmayan bazı alıcılar çalışılmaktadır. öncelikle, yanıp sönen alıcılar ve çip ayırtaç gibi çok karmaşık olmayan alıcılar sunulmaktadır. Bu alıcılar için gereksinimler ve daha iyi performans sağlamaları için gerekli koşullar tartışılmaktadır. Daha sonra, doğrusal en düşük ortalama karesel hatalı alıcı ve bunu gerçekleştirmek için gereksinimler sunulmaktadır. Son olarak, hesaplama karmaşıklığı en çok olan ve diğer alıcılardan daha çok gereksinimi olan, optimal en büyük olabilirlik sezicisi elde edilmektedir. Kuramsal sonuçları onaylamak ve alıcıların performansını kıyaslamak için benzetim sonuçları gerçekleştirilmektedir.

ACKNOWLEDGMENTS

I would like to express my appreciation to my supervisor Asst. Prof. Dr. Sinan Gezici for his time, patience, understanding and encouragement. Also I would like to thank Prof. Orhan Arıkan and Asst. Prof. Dr. İbrahim Körpeoğlu for serving on my committee and reviewing my thesis.

Contents

List of Figures

List of Tables

Dedicated to my dear nieces, İlknur and Hiranur.

Chapter 1

Introduction

1.1   Objectives and Contributions of the Thesis

Since the US Federal Communications Commission (FCC) allowed the limited use of ultra-wideband (UWB) technology [2], it has been regarded as a new alternative in communication systems. A UWB signal possesses a bandwidth larger than 500 MHz and can use the bands allocated to other systems due its low power spectral density. Due to their large bandwidth and high time resolution, UWB signals are considered as suitable for high-speed data transmission [3], and accurate range and location estimation [4, 5]. In addition, UWB systems can be used for low-to-medium data rate communication with low cost receivers.

In order to implement UWB systems, impulse radio (IR) systems can be employed [6]-[10]. In IR systems, a train of pulses with durations on the order of nanoseconds are transmitted. Each pulse resides in an interval called "frame", and a number frames are employed for each information symbol. The information symbol can be carried by the positions or amplitudes of pulses [11]. In multiple access environments, in order to prevent collisions and increase robustness against interfering users, pulses of each user are transmitted according to a time-hopping

(TH) sequence, which aims to decrease the probability of collision between pulses of different users [6]. In addition to data modulation scheme, each pulse has a polarity randomization code that provides additional robustness against multiple access interference and eliminates spectral lines that violates UWB spectral mask [2, 12].

In practice, each UWB pulse can reach a receiver via tens or even hundreds of paths in a multipath environment. Hence, to collect energy from multipath components, Rake receivers can be employed [13]. Due to the large number of fingers [14, 15] and high sampling requirements, implementation of Rake receivers is challenging for UWB systems. This complexity of the Rake receiver has motivated researchers to come up with an alternative solution that does not need strict channel estimation requirements.

In order to ease the strict requirements of channel estimation, transmitted-reference (TR) UWB systems are proposed [16]-[18]. In these types of systems, one reference pulse and one data pulse are sent in each frame. The reference pulse contains no information and its channel response is used at the receiver. On the other hand, the data pulse is modulated by the information symbol and separated by a time delay of D from the reference pulse. To estimate the transmitted information symbol, the receiver employs the received signal $r(t)$ and its time shifted version $r(t - D)$. However, the required analog delay element is commonly made by a coaxial cable and it is difficult to build it in a low power integrated receiver. For example, 20 ft of cable is needed for 20 nanoseconds of time delay [19].

Since TR UWB leads to miniaturization problems, another modulation scheme, which provides orthogonalization of data and reference signals in the frequency domain, namely frequency-shifted reference (FSR) UWB is proposed [20]. In FSR systems, frequency conversion is needed at the receiver instead of analog time delay. Hence, the receiver is significantly simpler than that in TR

systems. However, in order for the reference signal to serve as a reference for the data signal, the frequency shift between data and reference signals must be less than the coherence bandwidth [20]. Thus, FSR systems are employed for low data rate systems.

Since FSR systems have a data rate limitation, code-orthogonalized transmitted reference (COTR) or code-multiplexed transmitted-reference (CM-TR) UWB systems are proposed [21], [22]. In these types of systems, reference and data signals are transmitted with two distinct orthogonal codes. This feature also avoids detailed channel estimation and provides low complexity receivers similar to FSR. In addition there is no data rate limitation in these systems.

In Chapter 2 of this thesis, CM-TR systems are investigated and error probabilities for single and multiple user cases are computed. First, energy obtained from each frame is represented by chi-square random variables. Then, the decision rule for the information symbol reduces to the sign detection of the difference between two chi-square random variables. In the single user case, the pulses are transmitted in only $N_f/2$ frames. Hence, the problem reduces to the difference of two chi-square random variables, where one is a central and the other is a noncentral chi-square random variable. Then, a closed form expression for the probability of error is derived. In the multi-user case, it is difficult to obtain a closed form expression for the exact probability of error using the same approach. Instead, the fact that a chi-square random variable is the sum of the square of Gaussian random variables is exploited and for large values of degrees of freedom, a closed form expression is obtained based on the central limit theorem (CLT).

In Chapter 3 of this thesis, some optimal and suboptimal receivers are analyzed. First, low complexity receivers such as blinking receiver (BR) and chip discriminator are studied. These types of receivers discard (some) colliding pulses and estimate transmitted information based on uncorrupted or lightly corrupted pulses [23]-[24]. The conditions under which these receivers perform

well are discussed. Then, a linear MMSE receiver is analyzed, and its implementation requirements are discussed. Finally, as an optimal receiver, the maximum-likelihood (ML) detector is obtained, which minimizes the probability of error. This receiver is the most complex receiver among the studied ones and mainly serves as a reference for the other receivers.

In Chapter 4 of this thesis, simulation results are presented to verify the theoretical results. The channel statistics are taken from the IEEE 802.15.4a models, CM1, CM2, CM3, and CM4. For each channel model, the optimal integration interval is found and the simulations are performed by using those optimal intervals.

1.2   Organization of the Thesis

The organization of the thesis is as follows. In Chapter 2, CM-TR UWB systems are investigated and error probability expressions are computed. In the single user case, an exact error probability is obtained, while for the multi-user case an approximate closed form expression is derived.

In Chapter 3, some optimal and suboptimal receivers are analyzed and their implementation requirements are investigated.

In Chapter 4, in order to verify the theoretical results and t compare performance of various receivers, simulation results are presented.

Chapter 2

Performance Analysis of Conventional Receiver in Multipath Fading Channels

In this chapter, CM-TR UWB systems are investigated and performance of the conventional receiver is analyzed. First, a generic signal model that reduces to TR, FSR and CM-TR UWB systems in special cases is provided (Section 2.1). Then, the receiver structure is introduced and it is discussed that a CM-TR UWB system can be modeled as a generalized non-coherent pulse-position modulated system [1] (Section 2.2). Finally, the performance of the conventional receiver is analyzed and a closed form expression of the exact error probability is obtained for the single user case. Since it is difficult to derive an exact error probability for the multiuser case using the same approach, a closed form expression is obtained based on the Gaussian approximation (Section 2.3).

2.1 Signal Model

First, a generic signal structure that reduces to TR, FSR and CM-TR UWB signals in special cases is defined. The transmitted signal corresponding to the kth user is given as [1]

$$
s^{(k)}(t) = \sqrt{\frac{E_k}{2N_f}} \sum_{j=0}^{N_f-1} \left[a_j^{(k)} w\left(t - jT_f - c_j^{(k)}T_c\right) \right.
$$
$$
\left. + b^{(k)} a_j^{(k)} w\left(t - jT_f - c_j^{(k)}T_c - T_d\right) x(t) \right], \qquad (2.1)
$$

where T_f and T_c are, respectively, the frame and chip intervals, N_f is the number of frames per symbol, E_k is the symbol energy for user k, $w(t)$ is the UWB pulse with unit energy, and $b^{(k)} \in \{-1, +1\}$ is the binary information symbol for user k. In order to increase robustness against multiple access interference (MAI) and avoid spectral lines [12], pulses are modulated by polarity randomization codes $a_j^{(k)} \in \{-1, +1\}$, where $a_j^{(k)}$ and $a_i^{(l)}$ are independent for $(k, j) \neq (l, i)$. In order to prevent catastrophic collisions between pulses of different users, a time-hopping code $c_j^{(k)} \in \{0, 1, \ldots, N_c - 1\}$ is assigned to each user. Note that $c_j^{(k)}$ and $c_i^{(l)}$ are independent for $(k, j) \neq (l, i)$.

The signal model in (2.1) reduces to TR, FSR and CM-TR systems for specific values assigned to T_d and $x(t)$. For TR systems, T_d is time delay between the data pulse and the reference pulse, and $x(t) = 1$. For FSR systems, the orthogonalization is provided in the frequency domain and time shift is not needed. Hence, $T_d = 0$ and $x(t) = \sqrt{2}\cos(2\pi f_o t)$ are considered. For CM-TR systems, $T_d = 0$ and $x(t)$ is given by

$$
x(t) = \sum_{j=0}^{N_f-1} \tilde{d}_j^{(k)} p\left(t - jT_f\right), \qquad (2.2)
$$

where $p(t) = 1$ for $t \in [0, T_f]$ and $p(t) = 0$ otherwise, and $\tilde{d}_j^{(k)} \in \{-1, +1\}$ is the jth element of the code that provides orthogonalization of the data bearing signal and the reference signal for kth user.

From (2.2), (2.1) can be expressed as

$$s^{(k)}(t) = \sqrt{\frac{E_k}{2N_f}} \sum_{j=0}^{N_f-1} a_j^{(k)} (1 + b^{(k)} \tilde{d}_j^{(k)}) \, w(t - jT_f - c_j^{(k)} T_c) \; . \qquad (2.3)$$

Assume that the signal in (2.3) passes through an L-path channel. The channel impulse response can be written as

$$h_c(t) = \sum_{l=1}^{L} \alpha_l \, \delta(t - \tau_l) \; , \qquad (2.4)$$

where $\delta(t)$ is the Dirac delta function, and α_l and τ_l represent, respectively, the channel coefficient and delay of the lth path.

Considering K users and Gaussian noise, the received signal for the kth user can be expressed as

$$r_k(t) = \sqrt{\frac{E_k}{2N_f}} \sum_{j=0}^{N_f-1} a_j^{(k)} (1 + b^{(k)} \tilde{d}_j^{(k)}) \tilde{w}(t - jT_f - c_j^{(k)} T_c) + n(t) \; , \qquad (2.5)$$

where $\tilde{w}(t) = w(t) * h_c(t)$, and $n(t)$ is zero mean Gaussian noise with flat spectral density of σ^2 over the system bandwidth.

2.2   Receiver Structure

In order to estimate the transmitted information symbol corresponding to the kth user, $b^{(k)}$, from the received signal in (2.3), the conventional receiver can be used. The transmitted information symbol for the kth user employing the conventional receiver can be found as

$$\hat{b}^{(k)} = \text{sgn} \left\{ \int_0^{T_s} r^2(t) x(t) dt \right\} \; , \qquad (2.6)$$

where $\text{sgn}\{\cdot\}$ represents the sign operator and T_s is the symbol interval. From (2.2), (2.6) can also be expressed as

$$\hat{b} = \text{sgn} \left\{ \sum_{j=0}^{N_f-1} \tilde{d}_j^{(k)} \int_{jT_f}^{(j+1)T_f} r^2(t) dt \right\} \; . \qquad (2.7)$$

7

Let S_k and $\bar{S}_k$ represent the sets of frame indices for which $\tilde{d}_j^{(k)} = 1$ and $\tilde{d}_j^{(k)} = -1$, respectively; i.e.,

$$S_k = \{ j \in \mathcal{F} \,|\, \tilde{d}_j^{(k)} = 1 \} \tag{2.8}$$

$$\bar{S}_k = \{ j \in \mathcal{F} \,|\, \tilde{d}_j^{(k)} = -1 \} \tag{2.9}$$

where $\mathcal{F} = \{0, 1, \ldots, N_f - 1\}$ is the set of frame indices [1]. Note that, in (2.3), the orthogonalization codes for the reference pulses are set to 1 for all frames. Hence, in order to achieve orthogonality condition between reference and data signals, the condition

$$|S_k| = |\bar{S}_k| = N_f/2 \;, \tag{2.10}$$

where $S_k \cup \bar{S}_k = \mathcal{F}$, must be satisfied.

From (2.5), it is observed that, for $b^{(k)} = 1$, we transmit pulses in the frames indexed by S_k and the frames indexed by $\bar{S}_k$ contain no pulses. Similarly, for $b^{(k)} = -1$, we transmit pulses in the frames indexed by $\bar{S}_k$ and the frames indexed by S_k contain no pulses.

From (2.8) and (2.9), (2.7) can be expressed as

$$\sum_{j \in S_k} \int_{\Gamma_j} r^2(t)dt \mathop{\gtrless}_{\hat{b}^{(k)}=-1}^{\substack{\hat{b}^{(k)}=+1}} \sum_{j \in \bar{S}_k} \int_{\Gamma_j} r^2(t)dt \;, \tag{2.11}$$

which can be considered as a non-coherent detector for binary pulse position modulation (PPM) [1]. Note that, in (2.7), the integration over which the energy is calculated taken as T_f, whereas a generic expression is used in (2.11). If the TH sequence for the user of interest is known, then the integration interval can be chosen in an optimal manner, which will be discussed later.

2.3 Performance Analysis

2.3.1 Formulation

The expression in (2.11) can be written as the difference of two chi-square random variables as

$$D = \sum_{j \in S_k} \int_{\Gamma_j} r^2(t)dt - \sum_{j \in \bar{S}_k} \int_{\Gamma_j} r^2(t)dt \underset{\hat{b}^{(k)}=-1}{\overset{\hat{b}^{(k)}=+1}{\underset{<}{\gtrless}}} 0 \ . \tag{2.12}$$

Due to the presence of K users in the system, the received signal $r(t)$ can be expressed as

$$r(t) = \sum_{k=1}^{K} r_k(t) + n(t) \ , \tag{2.13}$$

where $n(t)$ is white Gaussian noise and $r_k(t)$ denoted the received signal for the kth user, which is given by

$$r_k(t) = \sqrt{\frac{E_k}{2N_f}} \sum_{j=0}^{N_f-1} a_j^{(k)}(1 + b^{(k)} \tilde{d}_j^{(k)}) \tilde{w}(t - jT_f - c_j^{(k)}T_c) \ . \tag{2.14}$$

Without loss of generality, user 1 is considered as the user of interest. Also, for $b^{(1)} \in \{-1, 1\}$ with equal probability, the probability of error can be expressed from (2.12) as

$$P_e = \frac{1}{2} P\left\{D > 0|b^{(1)} = -1\right\} + \frac{1}{2} P\left\{D \le 0|b^{(1)} = 1\right\} \ . \tag{2.15}$$

Assuming that the data bits are equally likely to be -1 or 1 for all users, the probability of error can be expressed as

$$P_e = \frac{1}{2^K} \sum_{\tilde{\mathbf{b}} \in \{\pm 1\}^{K-1}} \left(P\left\{D > 0|b^{(1)} = -1 \& \tilde{\mathbf{b}}\right\} + P\left\{D \le 0|b^{(1)} = 1 \& \tilde{\mathbf{b}}\right\} \right) , \tag{2.16}$$

where

$$\tilde{\mathbf{b}} \triangleq [b^{(2)} \cdots b^{(K)}]^T$$
$$\mathbf{b} \triangleq [b^{(1)} \cdots b^{(K)}]^T \ . \tag{2.17}$$

It is also possible to express P_e in (2.16) in terms of the conditional cumulative distribution function (CDF) of D, namely, $P\{D \leq 0|\mathbf{b}\} = F_{D|\mathbf{b}}(0)$ and $P\{D > 0|\mathbf{b}\} = 1 - F_{D|\mathbf{b}}(0)$.

Let $\tilde{r}(t) = \sum_{k=1}^{K} r_k(t)$ represent the sum of the received signals from all users. Then, (2.12) can be written as

$$D = \sum_{j \in S} \int_{\Gamma_j} (\tilde{r}(t) + n(t))^2 dt - \sum_{j \in \bar{S}} \int_{\Gamma_j} (\tilde{r}(t) + n(t))^2 dt \ . \tag{2.18}$$

Note that no subscripts are used with S and $\bar{S}$ for convenience, and S_1 and $\bar{S}_1$ are implied unless stated otherwise.

For a given set of information symbols $\mathbf{b}$, $\tilde{r}(t)$ is a deterministic quantity. Therefore, if we define random variables D_1 and D_2 as

$$D_1 = \sum_{j \in S} \int_{\Gamma_j} (\tilde{r}(t) + n(t))^2 dt \quad \text{and} \quad D_2 = \sum_{j \in \bar{S}} \int_{\Gamma_j} (\tilde{r}(t) + n(t))^2 dt \ , \tag{2.19}$$

then they are conditionally independent assuming that the noise realizations at different integration intervals are independent, which is approximately true in practice [1].

Since $n(t)$ is zero mean Gaussian noise with a flat spectral density of σ^2 over the system bandwidth, the energy samples from jth frame $\int_{\Gamma_j} (\tilde{r}(t) + n(t))^2 dt$ can be shown to be distributed as chi-square random variables [25]. Therefore, (2.18) can be represented as

$$D = \sum_{j \in S} \chi_M^2(\theta_j(\mathbf{b})) - \sum_{j \in \bar{S}} \chi_M^2(\theta_j(\mathbf{b})) \ , \tag{2.20}$$

where $\chi_M^2(\cdot)$ denotes a chi-square distributed random variable with M degrees of freedom, M is the approximate dimensionality of the signal space, which is obtained from the time-bandwidth product, and $\theta_j(\mathbf{b})$ is the signal energy in the jth frame (in the absence of noise) for a given set of binary information symbols

b. From (2.13) (2.14) and (2.18), $\theta_j(\mathbf{b})$ can be obtained as

$$\theta_j(\mathbf{b}) = \int_{\Gamma_j} \left(\sum_{k=1}^{K} \sqrt{\frac{E_k}{2N_f}} a_j^{(k)} (1 + b^{(k)} \tilde{d}_j^{(k)}) \, \tilde{w}(t - jT_f - c_j^{(k)} T_c) \right)^2 dt$$

$$= \sum_{k_1=1}^{K} \sum_{k_2=1}^{K} \frac{\sqrt{E_{k_1} E_{k_2}}}{2N_f} a_j^{(k_1)} a_j^{(k_2)} \left(1 + b^{(k_1)} \tilde{d}_j^{(k_1)} \right) \left(1 + b^{(k_2)} \tilde{d}_j^{(k_2)} \right)$$

$$\times R_{\tilde{w}}^j \left((c_j^{(k_1)} - c_j^{(k_2)}) T_c \right) , \tag{2.21}$$

where the last term $R_{\tilde{w}}^j(\cdot)$ can be considered as the correlation function between user k_1 and user k_2 in the jth frame and is defined as

$$R_{\tilde{w}}^j \left((c_j^{(k_1)} - c_j^{(k_2)}) T_c \right) = \int_{\Gamma_j} \tilde{w}(t - jT_f - c_j^{(k_1)} T_c) \, \tilde{w}(t - jT_f - c_j^{(k_2)} T_c) \, dt . \tag{2.22}$$

It follows from the definition of the chi-square distribution that the sum of independent chi-square random variables is also chi-square distributed. Therefore, (2.20) can be written as

$$D = D_1 - D_2 = \chi^2_{\frac{N_f M}{2}} \left(\sum_{j \in S} \theta_j(\mathbf{b}) \right) - \chi^2_{\frac{N_f M}{2}} \left(\sum_{j \in \bar{S}} \theta_j(\mathbf{b}) \right) , \tag{2.23}$$

since $|S| = |\bar{S}| = N_f/2$. For a given set of information symbols $\mathbf{b}$, the CDF of D can be found as

$$P\{D \leq 0|\mathbf{b}\} = P\{D_1 \leq D_2|\mathbf{b}\} = \int P\{D_1 \leq x|\mathbf{b}\} f_{D_2|\mathbf{b}}(x) dx$$

$$= \int F_{D_1|\mathbf{b}}(x) f_{D_2|\mathbf{b}}(x) \, dx , \tag{2.24}$$

where $f_{D_2|\mathbf{b}}(x)$ denotes the conditional probability density function (PDF) of D_2 given $\mathbf{b}$.

Define $\tilde{M} = MN_f/2$, $\tilde{\theta}_1 = \sum_{j \in S} \theta_j(\mathbf{b})$ and $\tilde{\theta}_2 = \sum_{j \in \bar{S}} \theta_j(\mathbf{b})$. Then, the conditional CDF of D_1 can be obtained after some manipulation (see Appendix A) as follows:

$$F_{D_1|\mathbf{b}}(x) = \sum_{j=0}^{\infty} e^{-\tilde{\theta}_1/(2\sigma^2)} \frac{(\tilde{\theta}_1/(2\sigma^2))^j}{j!} \frac{\gamma(j + \tilde{M}/2 \, , \, x/(2\sigma^2))}{\Gamma(j + \tilde{M}/2)} , \tag{2.25}$$

11

where $\Gamma(n) = (n-1)!$ for positive integer n is the gamma function [26], and $\gamma(k, z)$ is the lower incomplete gamma function [27]. Similarly, the conditional PDF of D_2 is calculated as

$$f_{D_2|\mathbf{b}}(x) = \frac{1}{2\sigma^2} e^{\frac{-(x+\tilde{\theta}_2)}{2\sigma^2}} \left(\frac{x}{\tilde{\theta}_2}\right)^{\frac{\tilde{M}}{4} - \frac{1}{2}} I_{\tilde{M}/2-1}\left(\frac{\sqrt{\tilde{\theta}_2 x}}{\sigma^2}\right), \qquad (2.26)$$

where $I_v(z)$ for $z \geq 0$ is the vth order modified Bessel function of the first kind [27].

Note that if $\tilde{\theta}_1 = 0$ and $\tilde{\theta}_2 = 0$, then D_1 and D_2 are distributed as central chi-square random variables, and the expressions above reduce, respectively, to

$$F_{D_1|\mathbf{b}}(x) = \frac{\gamma(\tilde{M}/2, x/2\sigma^2)}{\Gamma(\tilde{M}/2)} \quad \text{and} \quad f_{D_2|\mathbf{b}}(x) = \frac{x^{\tilde{M}/2-1}e^{-x/2\sigma^2}}{\sigma^{\tilde{M}}2^{\tilde{M}/2}\Gamma(\tilde{M}/2)}. \qquad (2.27)$$

2.3.2 Single User Case

In the single user case, $\mathbf{b} = b^{(1)}$ and the probability of error can be expressed as

$$P_e = \frac{1}{2} P\{D_1 > D_2 | b^{(1)} = -1\} + \frac{1}{2} P\{D_1 \leq D_2 | b^{(1)} = 1\}, \qquad (2.28)$$

where $b^{(1)} \in \{-1, +1\}$ with equal probability and D_1 and D_2 are as given in (2.19) with $\tilde{r}(t) = r_1(t)$.

Note that, for $b^{(1)} = -1$, we transmit the pulses in the frames indexed by $\bar{S}$, and the other frames contain no pulses. Thus, using (2.21), one can obtain

$$\theta_j(-1) = \begin{cases} 0, & \text{if } j \in S \\ \theta, & \text{if } j \in \bar{S} \end{cases} \qquad (2.29)$$

where

$$\theta \triangleq \frac{2E_1}{N_f} \int_{\Gamma_j} \tilde{w}^2(t)dt = \frac{2E_1 E_{\tilde{w}}}{N_f}. \qquad (2.30)$$

Then, from (2.23), D_1 and D_2 are distributed as follows:

$$D_1 \sim \chi^2_{\frac{MN_f}{2}}(0) \quad \text{and} \quad D_2 \sim \chi^2_{\frac{MN_f}{2}}(\theta N_f/2). \qquad (2.31)$$

Similarly, for $b^{(1)} = 1$,

$$D_1 \sim \chi^2_{\frac{MN_f}{2}}(\theta N_f/2) \quad \text{and} \quad D_2 \sim \chi^2_{\frac{MN_f}{2}}(0) . \tag{2.32}$$

From (2.31) and (2.32), the probability of error can be calculated based on (2.25)-(2.27) as

$$P_e = P\{D_1 > D_2 | b^{(1)} = -1\} = \int P\{D_1 > x | b^{(1)} = -1\} P\{D_2 = x | b^{(1)} = -1\} \, dx$$

$$= \int \left(1 - \frac{\gamma(\frac{MN_f}{4}, \frac{x}{2\sigma^2})}{\Gamma(\frac{MN_f}{4})}\right) \frac{1}{2\sigma^2} e^{-(x+\theta N_f/2)/2\sigma^2}$$

$$\times \left(\frac{x}{\theta N_f/2}\right)^{\frac{MN_f}{8} - \frac{1}{2}} I_{\frac{MN_f}{4} - 1}\left(\frac{\sqrt{x\theta N_f/2}}{\sigma^2}\right) \, dx . \tag{2.33}$$

Note that $P_e = P\{D_1 > D_2 | b^{(1)} = -1\}$ is used since $P\{D_1 > D_2 | b^{(1)} = -1\} = P\{D_1 \leq D_2 | b^{(1)} = 1\}$ in (2.28) due to symmetry.

The probability of error expression in (2.33) can be evaluated numerically, for example, in MATLAB. Although it provides an accurate expression for the probability of error, a simpler approximate expression can also be useful in some cases. To that aim, the Gaussian approximation is employed in the following in order to obtain a simpler expression.

Lemma 2.1: *In a single user system, for a given binary symbol $b^{(1)} \in \{-1, +1\}$, D_1 and D_2 are Gaussian distributed as follows:*

$$
\begin{aligned}
b^{(1)} = -1 \Rightarrow &\begin{cases} D_1 \sim \mathcal{N}\left(\sigma^2 \frac{N_f M}{2}, \sigma^4 N_f M\right) \\ D_2 \sim \mathcal{N}\left(\sigma^2 \frac{N_f M}{2} + \theta N_f/2, \sigma^4 N_f M + 2\sigma^2 \theta N_f\right) \end{cases} \\
b^{(1)} = 1 \Rightarrow &\begin{cases} D_1 \sim \mathcal{N}\left(\sigma^2 \frac{N_f M}{2} + \theta N_f/2, \sigma^4 N_f M + 2\sigma^2 \theta N_f\right) \\ D_2 \sim \mathcal{N}\left(\sigma^2 \frac{N_f M}{2}, \sigma^4 N_f M\right) \end{cases}
\end{aligned} . \tag{2.34}
$$

Proof: Please see Appendix B.

Note that for a given binary information symbol $b^{(1)}$, $D_1 - D_2$ is also Gaussian distributed based on the results in Lemma 2.1 as follows:

$$b^{(1)} = -1 \Rightarrow D_1 - D_2 \sim \mathcal{N}\left(-\theta N_f/2,\ 2\sigma^4 N_f M + 2\sigma^2 \theta N_f\right) \tag{2.35}$$

$$b^{(1)} = 1 \Rightarrow D_1 - D_2 \sim \mathcal{N}\left(\theta N_f/2,\ 2\sigma^4 N_f M + 2\sigma^2 \theta N_f\right) \tag{2.36}$$

Thus, from (2.28), the probability of error can be expressed as

$$P_e \approx Q\left(\frac{\theta N_f/2}{\sqrt{2\sigma^2 N_f(M\sigma^2 + \theta)}}\right), \tag{2.37}$$

which can also be stated, based on (2.29), as

$$P_e \approx Q\left(\frac{E_1 E_{\tilde{w}}}{\sqrt{2\sigma^2(N_f M\sigma^2 + 2E_1 E_{\tilde{w}})}}\right). \tag{2.38}$$

In order to compare the expressions in (2.33) and (2.38), some numerical evaluations are performed. Figures 2.1–2.5 plot the bit error probability (BEP) versus the signal-to-noise ratio (SNR) for different numbers of frames N_f. From the plots, it is observed that, for a constant symbol energy, the performance of the receiver degrades as N_f increases, which is expected from (2.38). Intuitively, the receiver collects more noise as N_f increases for a constant symbol energy. In addition, there is a good agreement between the exact theoretical results and the simulation results. However, the approximate theoretical results match closely to the simulation results only for large values of N_f. This can be explained by the fact that the Gaussian approximation assumes get accurate for large values of $MN_f/2$.
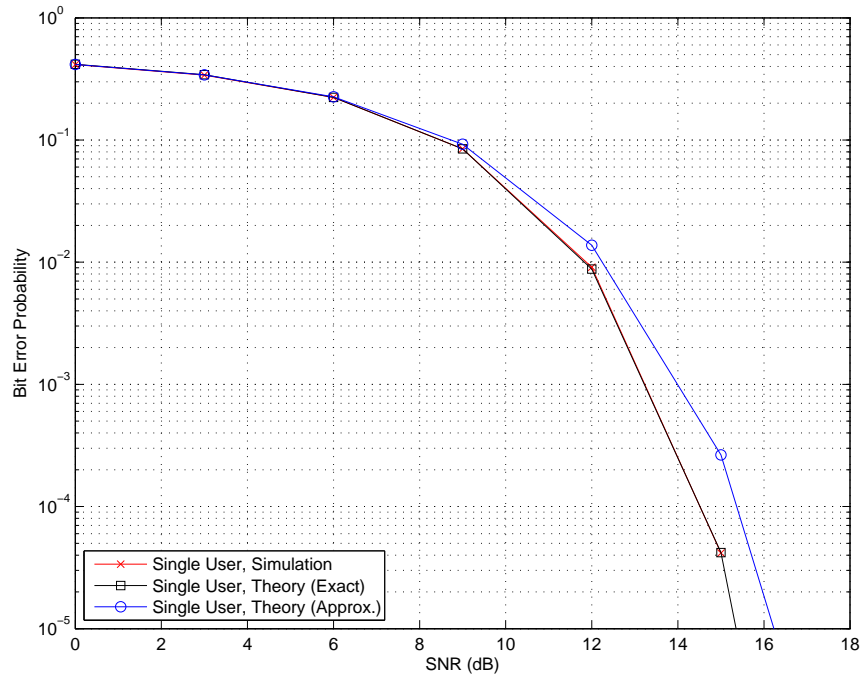
Figure 2.1: BEP versus SNR for a single user system with $N_f = 4$ and $E_1 = 1$.
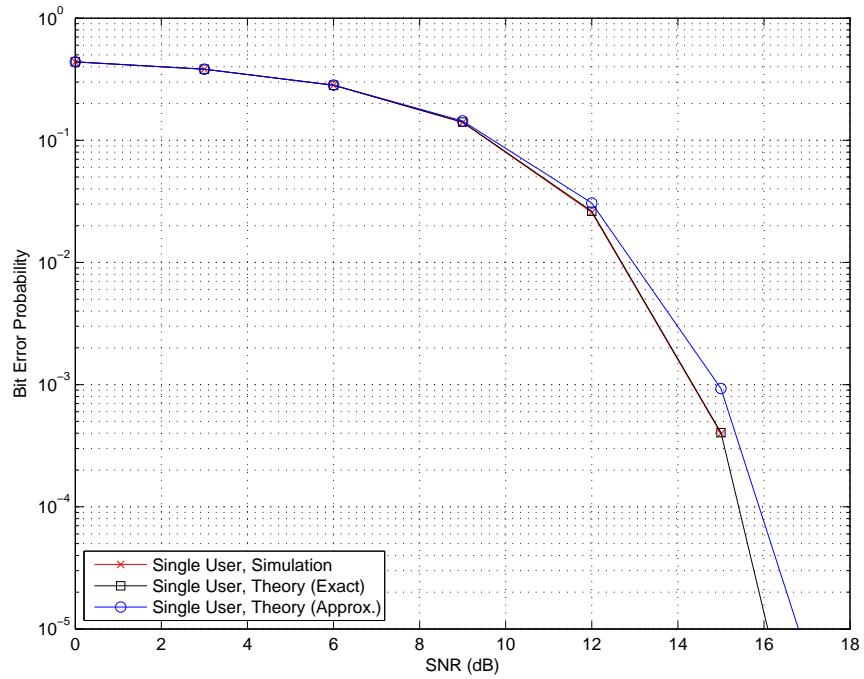
Figure 2.2: BEP versus SNR for a single user system with $N_f = 8$ and $E_1 = 1$.
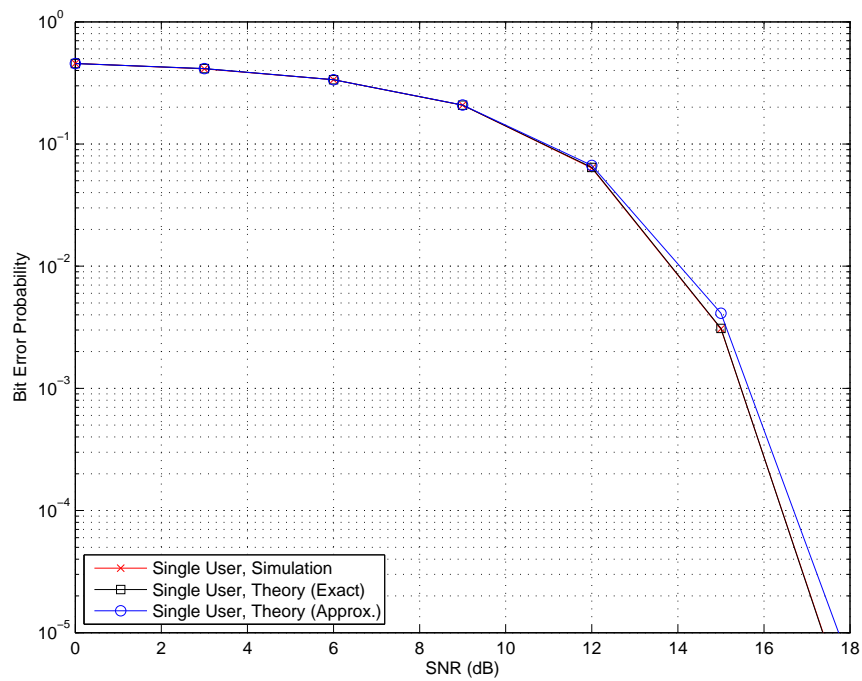
Figure 2.3: BEP versus SNR for a single user system with $N_f = 16$ and $E_1 = 1$.
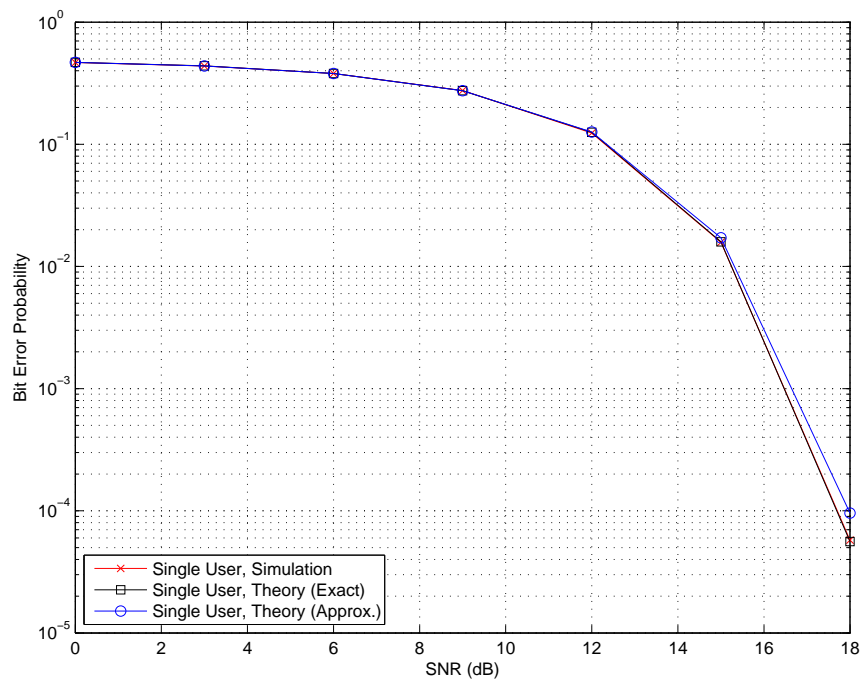
Figure 2.4: BEP versus SNR for a single user system with $N_f = 32$ and $E_1 = 1$.
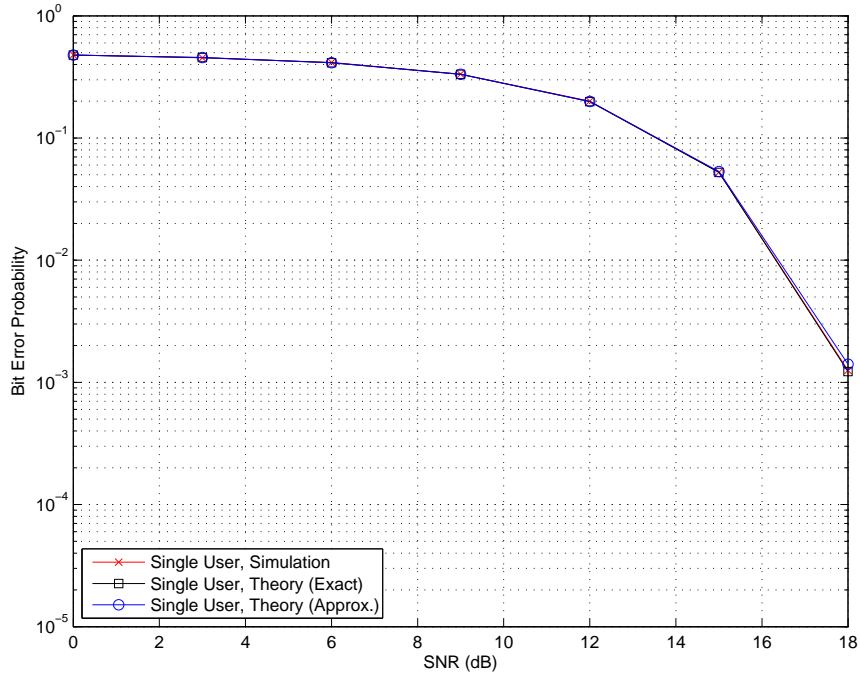
Figure 2.5: BEP versus SNR for a single user system with $N_f = 64$ and $E_1 = 1$.

In Figures 2.1–2.5, a single path channel is considered for simplicity, and the results are presented to verify the theoretical results (realistic multipath channels are considered in Chapter 4). Since a single path scenario is considered in the figures, the integration interval is taken as one pulse duration. Therefore, the degrees of freedom for the chi-square random variable in each frame is small since it is determined by the time duration and the bandwidth product. Therefore, the Gaussian approximation gets accurate only for large N_f values since the degrees of freedom of the decision variables are given by $MN_f/2$ as shown in (2.31) and (2.32). In practical UWB channels, there can be a large number of multipath components; hence, a larger integration interval is employed. Therefore, the Gaussian approximation can get more accurate in practice.

2.3.3 Multiuser Case

In this section, the performance of the conventional receiver is analyzed for in multiuser environments. Although it is difficult to obtain a reasonable expression of the exact probability of error, a closed form expression can be obtained based on the Gaussian approximation as in [28].

Without loss of generality, user 1 is assumed as the user of interest in a K-user system. Assuming equiprobable information symbols for all users, the probability of error can be expressed as

$$P_e = \frac{1}{2^K} \sum_{\tilde{\mathbf{b}} \in \{\pm 1\}^{K-1}} \left(P\left\{ D_1 - D_2 \geq 0 \mid b^{(1)} = -1, \tilde{\mathbf{b}} \right\} \right.$$

$$\left. + P\left\{ D_1 - D_2 < 0 \mid b^{(1)} = -1, \tilde{\mathbf{b}} \right\} \right), \qquad (2.39)$$

where $\tilde{\mathbf{b}} = [b^{(2)} \cdots b^{(K)}]^T$, and D_1 and D_2 are given as

$$D_1 = \sum_{j \in S} \chi_M^2(\theta_j(\mathbf{b})) \quad \text{and} \quad D_2 = \sum_{j \in \bar{S}} \chi_M^2(\theta_j(\mathbf{b})) . \qquad (2.40)$$

Note that $\chi_M^2(\theta_j(\mathbf{b}))$ is a noncentral chi-square random variable with M degrees of freedom and a noncentrality parameter of $\theta_j(\mathbf{b})$. Here, M is the approximate dimensionality of the signal space, which is obtained from the time-bandwidth product, and $\theta_j(\mathbf{b})$ denotes the energy obtained from jth frame (in the absence of noise) for information bits $\mathbf{b} = [b^{(1)} \cdots b^{(K)}]^T$ (see (2.21)).

In the following lemma, the asymptotical normality of D_1 and D_2 is shown similarly to [28].

Lemma 2.2: *As $MN_f \to \infty$, D_1 and D_2 are Gaussian distributed as follows:*

$$D_1 \sim \mathcal{N}\left(\sum_{j \in S} (\sigma^2 M + \theta_j(\mathbf{b})), \sum_{j \in S} (2M\sigma^4 + 4\sigma^2 \theta_j(\mathbf{b})) \right) ,$$

$$D_2 \sim \mathcal{N}\left(\sum_{j \in \bar{S}} (\sigma^2 M + \theta_j(\mathbf{b})), \sum_{j \in \bar{S}} (2M\sigma^4 + 4\sigma^2 \theta_j(\mathbf{b})) \right) . \qquad (2.41)$$

Proof: Please see Appendix B.

Since $|S| = |\bar{S}| = N_f/2$, and the difference of two Gaussian random variables is also Gaussian, the term $D_1 - D_2$ is normally distributed as

$$D_1 - D_2 \sim \mathcal{N} \left(\sum_{j \in S} \theta_j(\mathbf{b}) - \sum_{j \in \bar{S}} \theta_j(\mathbf{b}), 2\sigma^4 M N_f + 4\sigma^2 \sum_{j=0}^{N_f-1} \theta_j(\mathbf{b}) \right) . \quad (2.42)$$

Then, the probability of error can be calculated from (2.39) as

$$P_e = \frac{1}{2^K} \sum_{\tilde{\mathbf{b}} \in \{\pm 1\}^{K-1}} \left\{ Q \left(\frac{\sum_{j \in \bar{S}} \theta_j(\tilde{\mathbf{b}},\ b^{(1)} = -1) - \sum_{j \in S} \theta_j(\tilde{\mathbf{b}},\ b^{(1)} = -1)}{\sqrt{2\sigma^4 M N_f + 4\sigma^2 \sum_{j=0}^{N_f-1} \theta_j(\tilde{\mathbf{b}},\ b^{(1)} = -1)}} \right) \right.$$

$$\left. + Q \left(\frac{\sum_{j \in S} \theta_j(\tilde{\mathbf{b}},\ b^{(1)} = 1) - \sum_{j \in \bar{S}} \theta_j(\tilde{\mathbf{b}},\ b^{(1)} = 1)}{\sqrt{2\sigma^4 M N_f + 4\sigma^2 \sum_{j=0}^{N_f-1} \theta_j(\tilde{\mathbf{b}},\ b^{(1)} = 1)}} \right) \right\} \quad (2.43)$$

Note that for the single user case; that is, $\mathbf{b} = b^{(1)}$, the expression above reduces to (2.38) as expected.

Chapter 3

Optimal and Suboptimal Receivers

In this chapter, some optimal and suboptimal receivers are studied for CM-TR UWB systems. First, low complexity receivers such as the blinking receiver (BR) and the chip discriminator are discussed (Section 3.1 and 3.2). The main idea behind these types of receivers is to discard some of the colliding pulses of the user of interest and to estimate the transmitted information symbol based on uncorrupted or slightly corrupted pulses. If the number of pulses with slight or no collision is sufficiently high per information symbol, these two receivers perform quite well. In addition to those receivers, a linear MMSE receiver is analyzed and discussed (Section 3.3). This MMSE receiver needs some partial channel knowledge and it is more complex than the previously discussed receivers. Lastly, the ML detector is investigated and its exact and approximate calculations are discussed (Section 3.4). Although, the ML detector is more complex and impractical in many cases, it is optimal and serves as a reference.

3.1 Blinking Receiver (BR)

The BR estimates the transmitted information symbol of the user of interest (user 1) based on the set of energy samples obtained from different frames with no collision of pulses [23]. In this case, the transmitted information symbol for user 1 can be estimated as follows:

$$\frac{\sum\limits_{j \in S_1} \tilde{\beta}_j y_j}{\sum\limits_{j \in S_1} \tilde{\beta}_j} \underset{\hat{b}^{(1)}=-1}{\overset{\hat{b}^{(1)}=+1}{\underset{<}{\gtrless}}} \frac{\sum\limits_{j \in \bar{S}_1} \tilde{\beta}_j y_j}{\sum\limits_{j \in \bar{S}_1} \tilde{\beta}_j} \ , \tag{3.1}$$

where y_j is the energy sample from the jth frame, S_1 and $\bar{S}_1$ are as in (2.8) and (2.9), respectively, and the coefficients $\tilde{\beta}_j$ are given by

$$\tilde{\beta}_j = \begin{cases} 1 \,, & \text{if } \ |c_j^{(1)} - c_j^{(k)}| \geq T_{\text{ds}}/T_c \\ 0 \,, & \text{otherwise} \end{cases} \ , \tag{3.2}$$

with T_{ds} denoting the delay spread of the channel and T_c being the chip interval.

Note that this receiver requires the knowledge of collisions between the pulses of the user of interest and those of the interfering users. Therefore, this receiver is more complex than the conventional receiver. Note also that this receiver discards colliding pulses irrespective of the interference level. Thus, for channels with large delay spreads, this receiver may perform poorly. In the formulation, it is assumed that there occurs no inter-frame interference (IFI).

3.2 Chip Discriminator

In practice, there can be hundreds of echoes from multipath components and the channel delay spread can be significantly larger than the pulse duration in a UWB system. In such cases, the blinking receiver might be very inefficient, since it does not have any information about the energies of interferers. Instead, the chip discriminator can be considered. In the chip discriminator, the transmitted

21

information symbol for user 1 can be found as

$$\frac{\sum\limits_{j \in S_1} \tilde{\beta}_j y_j}{\sum\limits_{j \in S_1} \tilde{\beta}_j} \mathop{\gtrless}\limits_{\hat{b}^{(1)}=-1}^{\hat{b}^{(1)}=+1} \frac{\sum\limits_{j \in \bar{S}_1} \tilde{\beta}_j y_j}{\sum\limits_{j \in \bar{S}_1} \tilde{\beta}_j} \ , \tag{3.3}$$

where y_j is the energy obtained from the jth frame and the coefficients $\tilde{\beta}_j$ are given by

$$\tilde{\beta}_j = \begin{cases} 1 & \text{if } |c_j^{(1)} - c_j^{(k)}| \geq \Delta_c \quad \text{or} \quad \frac{A_k}{A_1} \leq T \\ 0 & \text{otherwise} \end{cases} \ , \tag{3.4}$$

where Δ_c is the threshold for the difference between the time-hoping (TH) codes of user-1 and user-k, and T is the threshold for the ratio between the amplitude of the kth user (A_k) and the user of interest (A_1). By setting threshold values T and Δ_c, the colliding pulses with strong interferers are eliminated. In other words, the pulses with low levels of interference are taken into account as well. It should be noted that depending on the number of frames (N_f), Δ_c and T values, the terms $\sum_{j \in S} \tilde{\beta}_j$ or $\sum_{j \in \bar{S}} \tilde{\beta}_j$ in (3.3) might be zero in some cases. In such scenarios, the conventional receiver ($\tilde{\beta}_j = 1, \ j = 0, \ldots, N_f - 1$) might be used. Then, if the number of pulses per information symbol, $N_f/2$, is low, this receiver might perform closely to the conventional receiver.

In order to implement this receiver, only TH sequences and symbol energies of all users are needed and two threshold levels must be determined. The performance of this detector can be improved by setting threshold T based on the interfering energy. However, this requires detailed channel information, hence, a more complex receiver structure.

In Table 3.1, the optimal threshold values are shown for an example two-user scenario, in which the user energies are $E_1 = 1$ and $E_2 = 2$. The channel models CM1, CM2, CM3, and CM4 are as defined in [29].

Table 3.1: Optimal threshold values for CM1, CM2, CM3 and CM4 channel models in a 2-user system ($E_1 = 1$ and $E_2 = 2$) with $T_c = 1$ ns and SNR $= 12$ dB.

	CM1	CM2	CM3	CM4
Optimal value of Δ_c	25	25	12	20

3.3 Linear MMSE

In this section, the linear MMSE receiver is obtained. Let $y_j = \int_{\Gamma_j} r^2(t)dt, \quad j = 0, 1, \ldots, N_f - 1$, represent the set of energy samples obtained from the N_f frames. Assuming user 1 as the user of interest, y_j can be expressed as

$$
y_j = \int_{\Gamma_j} \left[r_1(t) + r_I(t) + n(t) \right]^2 dt
$$

$$
= \int_{\Gamma_j} [r_1(t)]^2 \, dt + 2 \int_{\Gamma_j} r_1(t) \left[r_I(t) + n(t) \right]^2 dt + \int_{\Gamma_j} \left[r_I(t) + n(t) \right]^2 dt , \quad (3.5)
$$

where $n(t)$ is the Gaussian noise and $r_I(t)$ is the sum of all interfering signals given by

$$
r_I(t) = \sum_{k=2}^{K} r_k(t) . \tag{3.6}
$$

The received signal from user-k during the jth frame can be expressed as

$$
r_k^j(t) = \sqrt{\frac{E_k}{2N_f}} a_j^{(k)} (1 + b^{(k)} \tilde{d}_j^{(k)}) \tilde{w}(t - jT_f - c_j^{(k)} T_c) \quad \text{for } t \in [jT_f, (j+1)T_f) . \tag{3.7}
$$

From (3.7), (3.5) can be written as

$$y_j = \frac{E_1}{2N_f}(2 + 2b^{(1)}\tilde{d}_j^{(1)}) \int_{\Gamma_j} \tilde{w}^2(t - jT_f - c_j^{(1)}T_c)dt$$

$$+ 2\sqrt{\frac{E_1}{2N_f}}a_j^{(1)}(1 + b^{(1)}\tilde{d}_j^{(1)}) \int_{\Gamma_j} \tilde{w}(t - jT_f - c_j^{(1)}T_c)[r_I(t) + n(t)]dt$$

$$+ \int_{\Gamma_j} [r_I(t) + n(t)]^2 dt .$$

To simplify the notation, the expression above can be written as

$$y_j = \frac{E_1\gamma_j^{(1)}}{N_f} + b^{(1)}\alpha_j + n_j , \tag{3.8}$$

where

$$\gamma_j^{(1)} = \int_{\Gamma_j} \tilde{w}^2(t - jT_f - c_j^{(1)}T_c)dt \tag{3.9}$$

$$\alpha_j = \frac{E_1\gamma_j^{(1)}}{N_f}\tilde{d}_j^{(1)} + \sqrt{\frac{2E_1}{N_f}}a_j^{(1)}\tilde{d}_j^{(1)} \int_{\Gamma_j} \tilde{w}(t - jT_f - c_j^{(1)}T_c)[r_I(t) + n(t)]dt \tag{3.10}$$

$$n_j = \sqrt{\frac{2E_1}{N_f}}a_j^{(1)} \int_{\Gamma_j} \tilde{w}(t - jT_f - c_j^{(1)}T_c)[r_I(t) + n(t)]dt + \int_{\Gamma_j} [r_I(t) + n(t)]^2 dt .$$

$$\tag{3.11}$$

It should be noted that $\gamma_j^{(1)} = E_{\tilde{w}}$ if Γ_j includes all the multipaths.

Considering all the frames from 0 to $N_f - 1$, (3.8) can be generalized as

$$\mathbf{y} = \mathbf{k} + b^{(1)}\boldsymbol{\alpha} + \mathbf{n} , \tag{3.12}$$

where

$$\mathbf{k} \triangleq \frac{E_1}{N_f} \left[\gamma_0^{(1)} \cdots \gamma_{N_f-1}^{(1)}\right]^T \tag{3.13}$$

$$\boldsymbol{\alpha} \triangleq [\alpha_0 \cdots \alpha_{N_f-1}]^T \tag{3.14}$$

$$\mathbf{n} \triangleq [n_0 \cdots n_{N_f-1}]^T . \tag{3.15}$$

In the linear MMSE receiver, the information symbol is estimated as [30]

$$\hat{b}^{(1)} = \text{sgn}\left\{\boldsymbol{\theta}_{\text{MMSE}}^T\mathbf{y}\right\} , \tag{3.16}$$

where

$$\boldsymbol{\theta}_{\mathrm{MMSE}} = \arg\min_{\boldsymbol{\theta}} E\left\{\left(\boldsymbol{\theta}^T\mathbf{y} - b^{(1)}\right)^2\right\}$$

$$= \left(E\left\{\mathbf{y}\mathbf{y}^T\right\}\right)^{-1} E\left\{\boldsymbol{\alpha}\right\}$$

$$= \left(\mathbf{k}\mathbf{k}^T + E\left\{\mathbf{n}\right\}\mathbf{k}^T + \mathbf{k}E\left\{\mathbf{n}^T\right\} + E\left\{\boldsymbol{\alpha}\boldsymbol{\alpha}^T\right\} + E\left\{\mathbf{n}\mathbf{n}^T\right\}\right)^{-1} E\left\{\boldsymbol{\alpha}\right\} \ .$$

(3.17)

The closed-form expressions for the terms in (3.17) are obtained in the following lemmas.

Lemma 3.1: *Let the polarity randomization codes, $a_j^{(k)}$, $k = 2,\ldots,K$ be i.i.d. random variables that take values ± 1 with equal probability. Then, $E\left\{n_j\right\}$ can be obtained as*

$$E\left\{n_j\right\} = \sum_{k=2}^{K} \frac{E_k}{N_f}\chi_{j,k} + |\Gamma_j|\,2B\sigma^2 \ ,$$

(3.18)

where $|\Gamma_j|$ denotes the length of the integration interval in the jth frame, and

$$\chi_{j,k} \triangleq \int_{\Gamma_j} \left[\tilde{w}\left(t - jT_f - c_j^{(k)}T_c\right)\right]^2 dt \ .$$

(3.19)

Proof: Please see Appendix C.

Lemma 3.2: *Let the polarity randomization codes, $a_j^{(k)}$, $k = 2,\ldots,K$ be i.i.d. random variables that take values ± 1 with equal probability. Then, $E\left\{n_j n_l\right\}$ can be expressed as*

$$E\left\{n_j n_l\right\} = \begin{cases} 4B^2\sigma^4\,|\Gamma|^2\left(1 + \frac{1}{B|\Gamma|}\right) + \sum_{k=2}^{K}\frac{E_k^2}{N_f^2}\left(1 + d_j^{(k)}d_l^{(k)}\right)\chi_{j,k_1}\chi_{l,k_2} \\[2mm] +2B\sigma^2\,|\Gamma|\sum_{k=2}^{K}\frac{E_k}{N_f}\left(\chi_{j,k} + \chi_{l,k}\right) \\[2mm] +\sum_{k_1\neq k_2}\frac{E_{k_1}E_{k_2}}{N_f^2}\chi_{j,k_1}\chi_{l,k_2} \ , \hspace{3cm} j \neq l \\[8mm] 4B^2\sigma^4\,|\Gamma|^2\left(1 + \frac{1}{B|\Gamma|}\right) + \sum_{k=2}^{K}\frac{2E_k^2}{N_f^2}\left(\chi_{j,k}\right)^2 + 4\sigma^2\sum_{k=2}^{K}\frac{E_k}{N_f}\left(B\,|\Gamma| + 1\right)\chi_{j,k} \\[2mm] +\sum_{k_1\neq k_2}\frac{E_{k_1}E_{k_2}}{N_f^2}\left(\chi_{j,k_1}\chi_{j,k_2} + 2\left[R_{\tilde{w}}^j((c_j^{(k_1)} - c_j^{(k_2)})T_c)\right]^2\right) \\[2mm] +\frac{2E_1}{N_f}\left[\sum_{k=2}^{K}\frac{E_k}{N_f}\left[R_{\tilde{w}}^j((c_j^{(1)} - c_j^{(k)})T_c)\right]^2 + \sigma^2\gamma_j^{(1)}\right] , \hspace{0.8cm} j = l \end{cases}$$

(3.20)

where $|\Gamma|$ denotes the common integration interval for all the frames.

Proof: Please see Appendix D.

Lemma 3.3: *Let the polarity randomization codes, $a_j^{(k)}$, $k = 2, \ldots, K$ be i.i.d. random variables that take value ± 1 with equal probability. Then, $E\{\alpha_j \alpha_l\}$ can be found as*

$$E\{\alpha_j \alpha_l\} = \begin{cases} \dfrac{E_1^2}{N_f^2} \gamma_j^{(1)} \gamma_l^{(1)} d_j^{(1)} d_l^{(1)} \, , & j \neq l \\[6mm] \dfrac{E_1^2}{N_f^2} \left(\chi_{j,k}\right)^2 + \dfrac{2E_1}{N_f} \left[\displaystyle\sum_{k=2}^{K} \dfrac{E_k}{N_f} \left[R_{\tilde{w}}^j((c_j^{(1)} - c_j^{(k)})T_c) \right]^2 + \sigma^2 \gamma_j^{(1)} \right] \, , & j = l \end{cases}$$

$$\tag{3.21}$$

Proof: Please see Appendix E.

Note that $E\{\mathbf{y}\mathbf{y}^T\}$ in (3.17) can be estimated from the previous observations in practice. Also, for polarity randomization codes $a_j^{(k)} \in \{-1, +1\}$ being equally likely,

$$E\{\alpha_j\} = \frac{E_1 \gamma_j^{(1)}}{N_f} \tilde{d}_j^{(1)} \, , \tag{3.22}$$

where $\gamma_j^{(1)}$ is given in (3.9). Thus, in order to implement this MMSE receiver, the symbol energy, the TH sequence and the orthogonalization codes of the user of interest (user 1) and $\gamma_j^{(1)}$ must be known. Moreover, the implementation of this receiver requires a matrix inversion. Therefore, the MMSE receiver is more complex than the BR, the chip discriminator, and the conventional receiver.

Note also that the information symbol can be estimated based on Lemmas 3.1–3.3 for the theoretical evaluation of the MMSE receiver. In this case, the knowledge of the symbol energies, the TH sequences and the orthogonalization codes for all users is required. In addition, the channel state information, the bandwidth of the receive filter and the integration interval should be known for those theoretical evaluations.

3.4　Maximum-Likelihood (ML) Detector

In order to compare the receivers discussed previously, the maximum-likelihood (ML) detector is chosen as a reference. This receiver might be considered as impractical, since it searches over 2^K hypotheses. However, it minimizes the probability of error and serves as an optimal receiver. In the ML detector, the set of information symbols $\mathbf{b} = [b^{(1)}...b^{(K)}]^{\mathrm{T}}$ is estimated as

$$\hat{\mathbf{b}} = \arg \max_{\mathbf{b}} p_{\mathbf{b}}(\mathbf{y}) = \arg \max_{\mathbf{b}} \prod_{j=0}^{N_f-1} p_{\mathbf{b}}(y_j) \ . \tag{3.23}$$

Taking the logarithm, we obtain

$$\hat{\mathbf{b}} = \arg \max_{\mathbf{b}} \log\left(p_{\mathbf{b}}(\mathbf{y})\right) = \arg \max_{\mathbf{b}} \sum_{j=0}^{N_f-1} \log\left(p_{\mathbf{b}}(y_j)\right) \ , \tag{3.24}$$

where $p_{\mathbf{b}}(y_j)$ is non-central chi-square distributed and given by

$$p_{\mathbf{b}}(y_j) = \frac{1}{2\sigma^2} \left(\frac{y_j}{\theta_j(\mathbf{b})}\right)^{\frac{M}{4}-\frac{1}{2}} e^{-\frac{\left(\theta_j(\mathbf{b})+y_j\right)}{2\sigma^2}} I_{\frac{M}{2}-1}\left(\frac{\sqrt{\theta_j(\mathbf{b})y_j}}{\sigma^2}\right) \ . \tag{3.25}$$

Note that, for a given set of binary information symbols $\mathbf{b}$, if the signal energy (in the absence of noise) is zero; that is, $\theta_j(\mathbf{b}) = 0$, then y_j is central chi-square distributed and $p_{\mathbf{b}}(y_j)$ given above reduces to

$$p_b(y_j) = \frac{y_j^{\frac{M}{2}-1} e^{\frac{y_j}{2\sigma^2}}}{\sigma^M 2^{\frac{m}{2}} \Gamma(M/2)} \ . \tag{3.26}$$

From (3.25), (3.24) can be expressed as

$$\arg \max_{\mathbf{b}} \sum_{j=0}^{N_f-1} \left(\frac{M}{4} - \frac{1}{2}\right) \left[\log y_j - \log\left(\theta_j(\mathbf{b})\right)\right]$$

$$- \frac{\left(\theta_j(\mathbf{b}) + y_j\right)}{2\sigma^2} + \log\left\{I_{\frac{M}{2}-1}\left(\frac{\sqrt{\theta_j(\mathbf{b})y_j}}{\sigma^2}\right)\right\} \ . \tag{3.27}$$

The expression in (3.27) provides an exact expression for the ML detector. However, the objective function can be computationally complex to evaluate. Therefore, the Gaussian approximation is used to provide a simpler alternative solution.

In Chapter 2, it has been observed that the Gaussian approximation can be employed for large values of M. Hence, the PDF of y_j can be written as

$$p_{\mathbf{b}}(y_j) = \frac{1}{\sqrt{2\pi}\sigma_j} e^{-\frac{(y_j - \mu_j)^2}{2\sigma_j^2}} , \qquad (3.28)$$

where μ_j and σ_j are given respectively by

$$\mu_j = \sigma^2 M + \theta_j(\mathbf{b}) , \qquad (3.29)$$

$$\sigma_j = 2M\sigma^4 + 4\sigma^2\theta_j(\mathbf{b}) . \qquad (3.30)$$

Thus, (3.24) can be expressed alternatively as

$$\arg \max_{\mathbf{b}} \log\left(p_{\mathbf{b}}(\mathbf{y})\right) = \arg \max_{\mathbf{b}} \sum_{j=0}^{N_f-1} \log\left(p_{\mathbf{b}}(y_j)\right)$$

$$= \arg \min_{\mathbf{b}} \sum_{j=0}^{N_f-1} \left\{ \log(\sqrt{2\pi}\sigma_j) + \frac{(y_j - \mu_j)^2}{2\sigma_j^2} \right\} . \qquad (3.31)$$

Note that in order to implement this detector, the channel state information, the TH sequences, the polarity and orthogonalization codes for all users must be known. This ML receiver is the most complex receiver among all the receivers discussed in this study and serves as a reference.

As a special case, the ML detector can be investigated in a single user scenario. In this case, (3.24) reduces to the Bayes decision rule, which, for equiprobable information symbols and uniform cost assignment, can be expressed as [1]

$$\prod_{j \in S} y_j^{\frac{1}{2} - \frac{M}{4}} I_{\frac{M}{2}-1}\left(\frac{\sqrt{\theta y_j}}{\sigma^2}\right) \underset{\hat{b}=-1}{\overset{\hat{b}=+1}{\underset{<}{\gtrless}}} \prod_{j \in \bar{S}} y_j^{\frac{1}{2} - \frac{M}{4}} I_{\frac{M}{2}-1}\left(\frac{\sqrt{\theta y_j}}{\sigma^2}\right) . \qquad (3.32)$$

Note that the Bayes rule in (3.32) also gives the minimum probability of error due to the assumption of uniform cost assignment [31]. In [1], it is shown that for large M values, the conventional receiver has nearly the same performance as the optimal receiver in (3.32). As an example, Figure 3.1 plots the BEP versus M for the conventional and the optimal receivers. From the plot, it is observed that the conventional receiver performs nearly optimally for $M \geq 8$. Note that the

degrees of freedom parameter, M, is determined by the product of the bandwidth and integration interval (Γ_j). In practice, due to a large number of multipath components, $B|\Gamma_j| \gg 1$ and the condition of $M \geq 8$ is commonly satisfied.

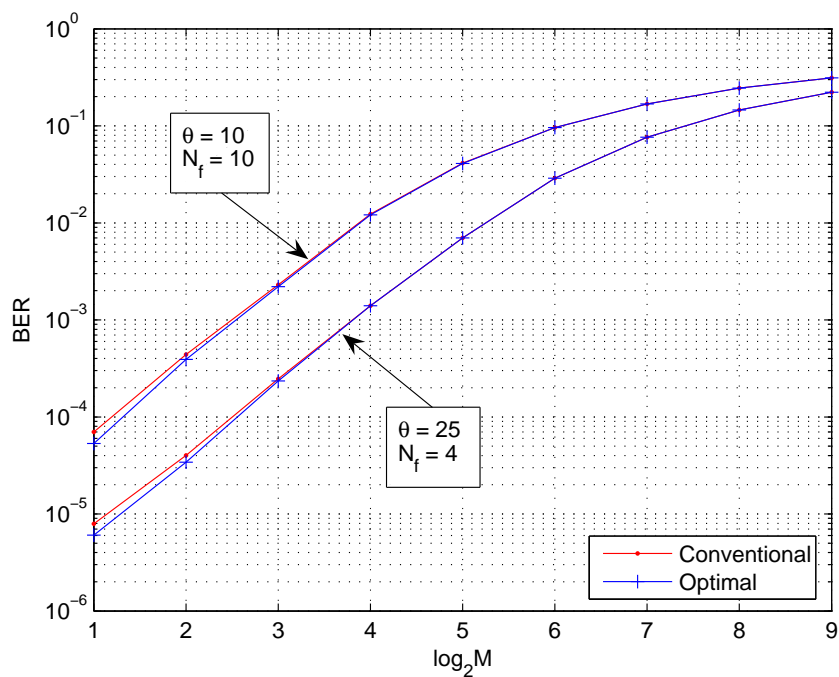Figure 3.1: BEP versus M for the conventional and the optimal receivers for the single user scenario [1].

Chapter 4

Simulation Studies

In this chapter, simulation results are presented in order to verify the theoretical results and to compare the performance of the receivers considered in the previous chapters. The UWB pulse $w(t)$ is chosen as the second order derivative of the Gaussian pulse [32]; that is,

$$w(t) = \left(1 - \frac{4\pi t^2}{\zeta^2}\right) e^{-\frac{2\pi t^2}{\zeta^2}} / \sqrt{E_p} \ , \tag{4.1}$$

where E_p is a scalar chosen to set $w(t)$ to unit energy and $\zeta = T_c/2.5$ determines the pulse width. An example of a unit energy pulse with $T_c = 1$ ns is illustrated in Figure 4.1. The bandwidth of the receive filter is 5 GHz and the channel statistics are taken from the IEEE 802.15.4a models CM1, CM2, CM3 and CM4 [29]. For the considered CM-TR UWB system, the system parameters are chosen as $N_f = 4$ and $N_c = 250$, which correspond to a data rate of $R_b = 1$ Mbit/s data rate.

In order to prevent catastrophic collisions between pulses of different users, TH sequences are employed for each user in each case. To avoid inter-frame interference (IFI), the TH sequences are chosen uniformly from the set $\{0, 1, \ldots, N_c - N_w\}$, where

$$N_w = \left\lceil \frac{T_w^{(i)}}{T_c} \right\rceil , \tag{4.2}$$

with $T_w^{(i)}$ being the duration of channel response to the pulse given in 4.1 for the ith channel model, T_c is chip duration (equal to 1 ns in the simulations) and $\lceil \cdot \rceil$ is the ceiling function. Table 4.1 indicates the values of N_w for different channel models and the sets from which the TH sequences are chosen to avoid IFI.

Table 4.1: TH sequence sets for CM1, CM2, CM3 and CM4 channel models.

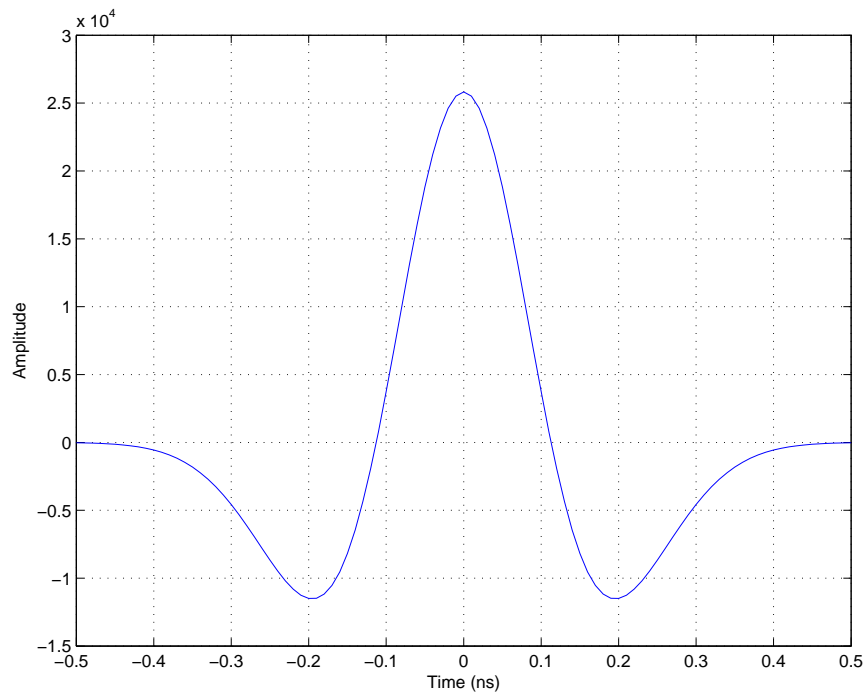| Channel Model	N_w	TH set
CM1	120	$c_j^{(k)} \in \{0, 1, \ldots, 130\}$
CM2	140	$c_j^{(k)} \in \{0, 1, \ldots, 110\}$
CM3	90	$c_j^{(k)} \in \{0, 1, \ldots, 160\}$
CM4	80	$c_j^{(k)} \in \{0, 1, \ldots, 170\}$

Figure 4.1: A UWB pulse with $T_c = 1$ns.

Due to the highly dispersive channel responses, the duration of the integration interval $|\Gamma|$ is critical and can affect the performance of the receivers significantly[1]. Figures 4.2–4.5 plot the BEP versus the integration interval $|\Gamma|$ for a two-user system for channel models CM1, CM2, CM3, and CM4, respectively. The integration intervals for the minimum probability of error is given in Table 4.2. From the plots and the table, it is observed that the performances of receivers are highly dependent on the integration interval $|\Gamma|$ and its optimal value is different for different receivers. Figures 4.6–4.9 plot the BEP versus the integration interval Γ, where the symbol energy of the interfering user is equal to 2. The integration intervals for the minimum probability of error are given in Table 4.3.
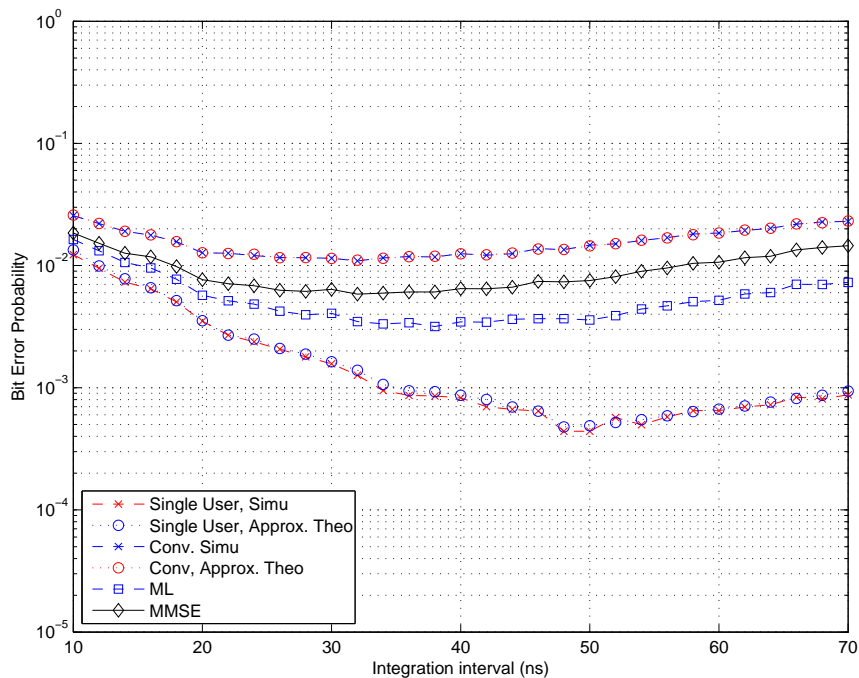

Figure 4.2: BEP versus $|\Gamma|$ for a 2-user system for CM1 with $N_f = 4$, $N_c = 250$ and $E_k = 1$ for $k = 1, 2$.

---

[1]For a given receiver structure, the same integration interval Γ is used for all the frames.

Figure 4.3: BEP versus $|\Gamma|$ for a 2-user system for CM2 with $N_f = 4$, $N_c = 250$ and $E_k = 1$ for $k = 1, 2$.

Figure 4.4: BEP versus $|\Gamma|$ for a 2-user system for CM3 with $N_f = 4$, $N_c = 250$ and $E_k = 1$ for $k = 1, 2$.
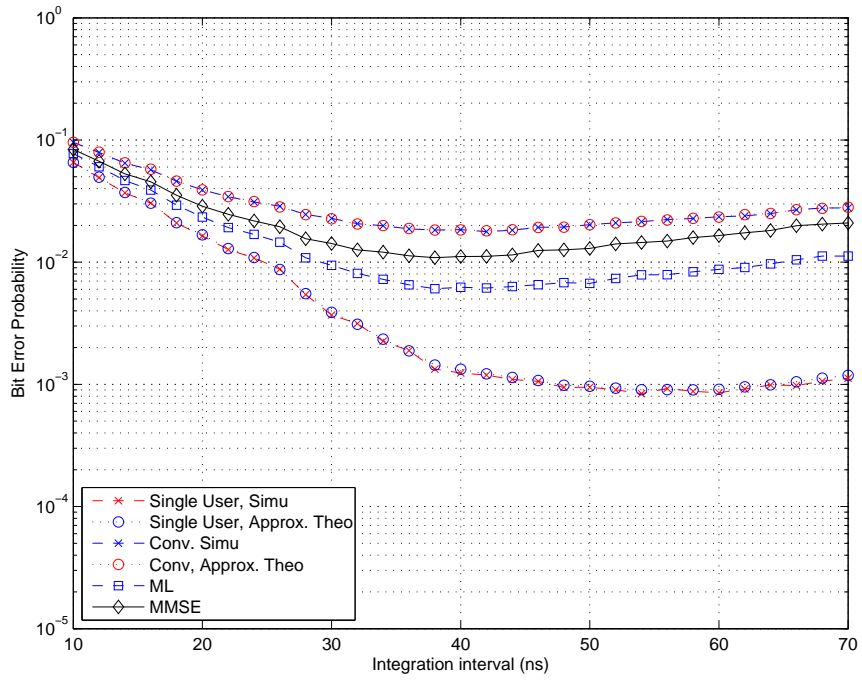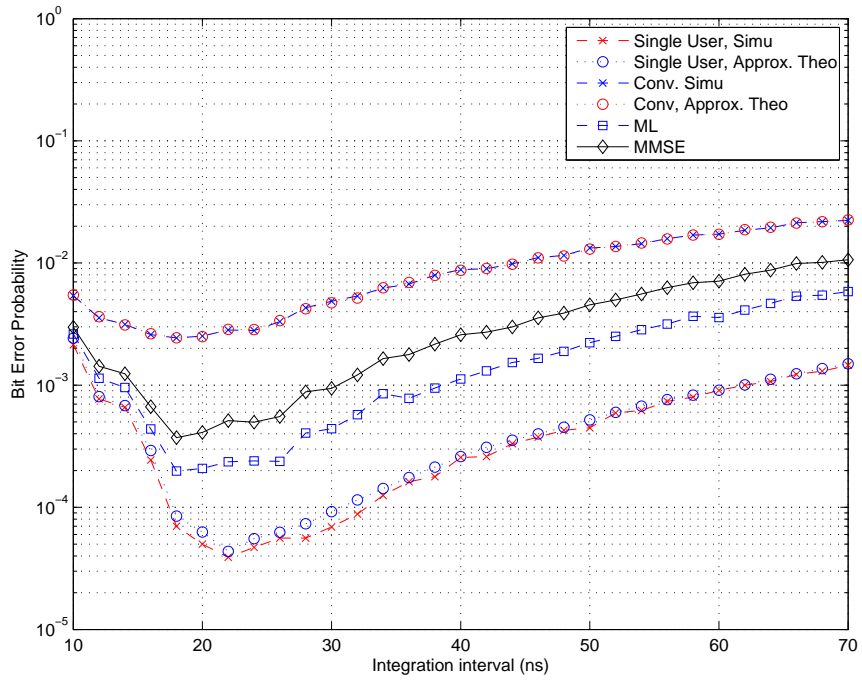
Figure 4.5: BEP versus $|\Gamma|$ for a 2-user system for CM4 with $N_f = 4$, $N_c = 250$ and $E_k = 1$ for $k = 1, 2$.

Figure 4.6: BEP versus $|\Gamma|$ for a 2-user system for CM1 with $N_f = 4$, $N_c = 250$, $E_1 = 1$ and $E_2 = 2$.

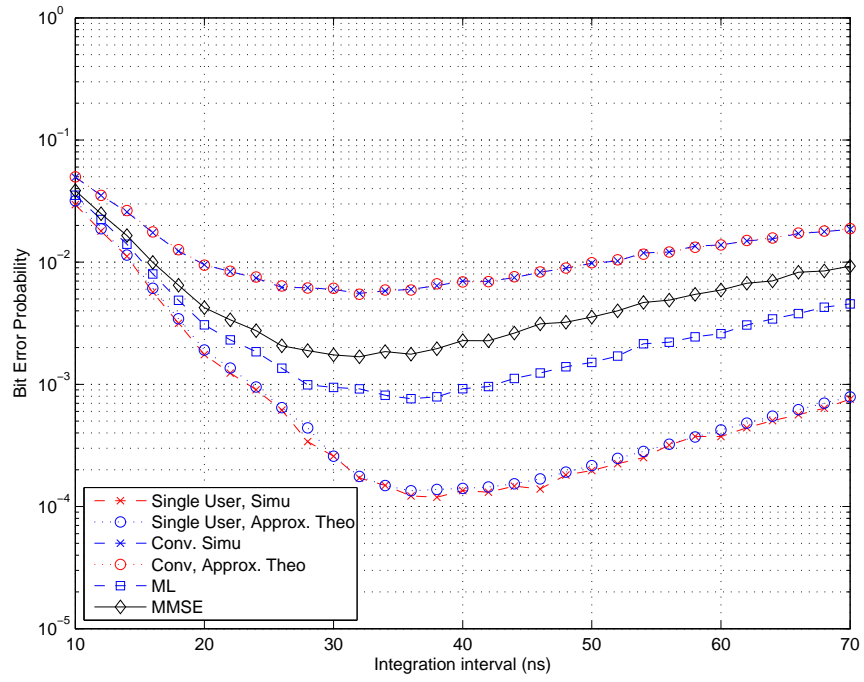Figure 4.7: BEP versus $|\Gamma|$ for a 2-user system for CM2 with $N_f = 4$, $N_c = 250$, $E_1 = 1$ and $E_2 = 2$.
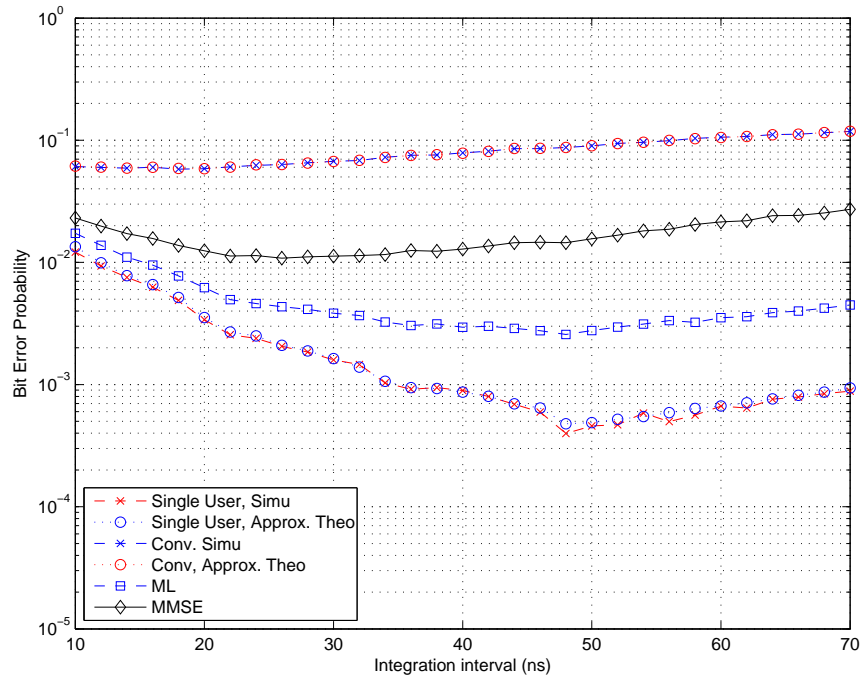

Figure 4.8: BEP versus $|\Gamma|$ for a 2-user system for CM3 with $N_f = 4$, $N_c = 250$, $E_1 = 1$ and $E_2 = 2$.

Figure 4.9: BEP versus $|\Gamma|$ for a 2-user system for CM4 with $N_f = 4$, $N_c = 250$, $E_1 = 1$ and $E_2 = 2$.

Table 4.2: Optimal integration intervals for CM1, CM2, CM3 and CM4 channel models in a 2-user system ($E_k = 1$, for $k = 1, 2$) with 12 dB SNR value. All the quantities are in nanosecond (ns).

Channel Model	Single User, Simu.	Single User, Theo.	Conv. Rec., Simu.	Conv. Rec., Theo.	MMSE Receiver	ML Detector
CM1	48	48	32	32	38	32
CM2	54	54	42	42	38	38
CM3	22	22	18	18	18	18
CM4	36	36	32	32	32	36

Table 4.3: Optimal integration intervals for CM1, CM2, CM3 and CM4 channel models in a 2-user system ($E_1 = 1$ and $E_2 = 2$) with 12 dB SNR value. All the quantities are in nanosecond (ns).

Channel Model	Single User, Simu.	Single User, Theo.	Conv. Rec., Simu.	Conv. Rec., Theo.	MMSE Receiver	ML Detector
CM1	48	48	18	18	26	48
CM2	54	54	32	32	36	46
CM3	22	22	10	10	18	22
CM4	36	36	20	20	30	36

Figure 4.10: BEP versus E_h/N_0 for a 2-user system for CM1 with $N_f = 4$, $N_c = 250$ and $E_k = 1$ for $k = 1, 2$.

Figure 4.11: BEP versus E_h/N_0 for a 2-user system for CM1 with $N_f = 4$, $N_c = 250$, $E_1 = 1$ and $E_2 = 2$.
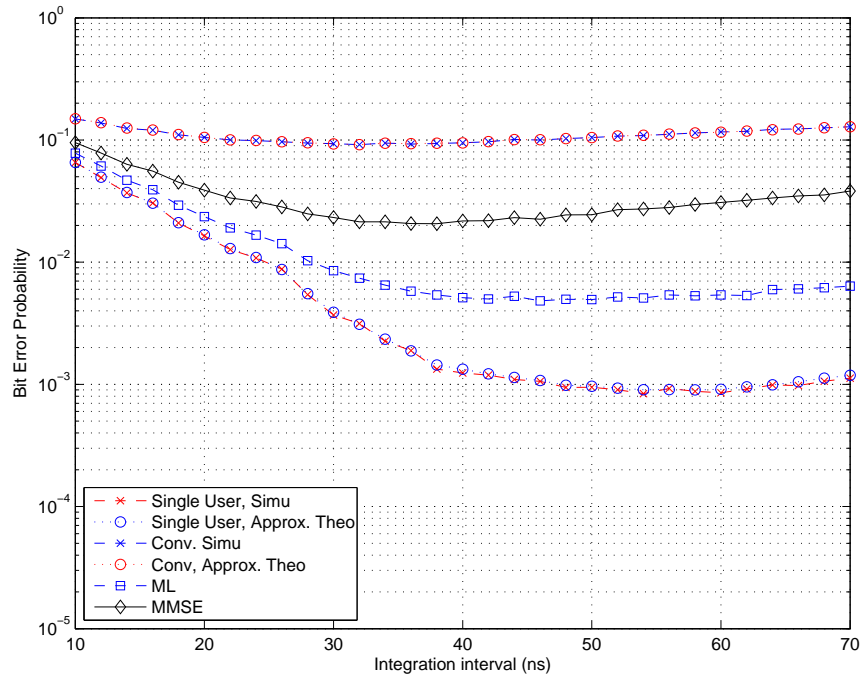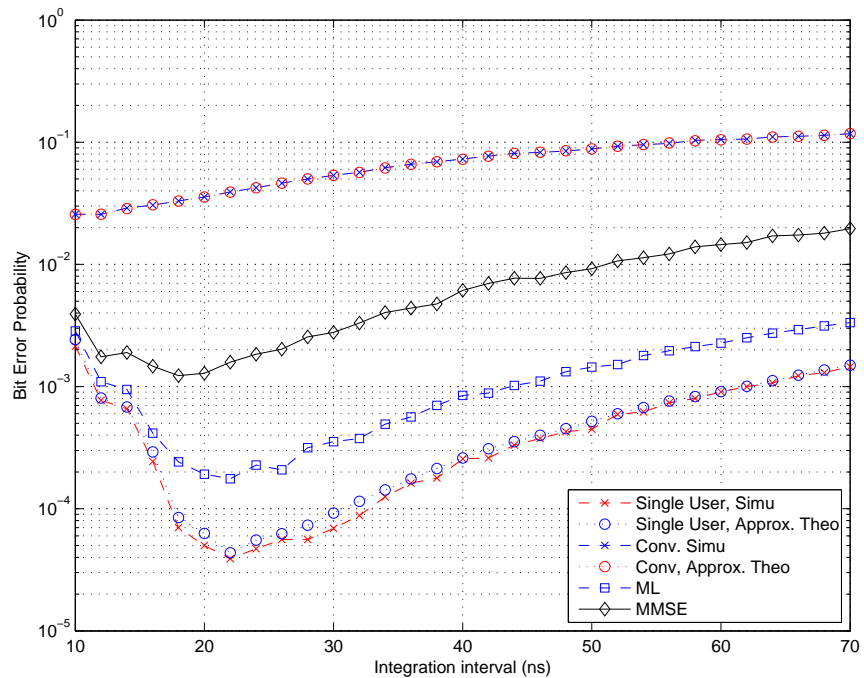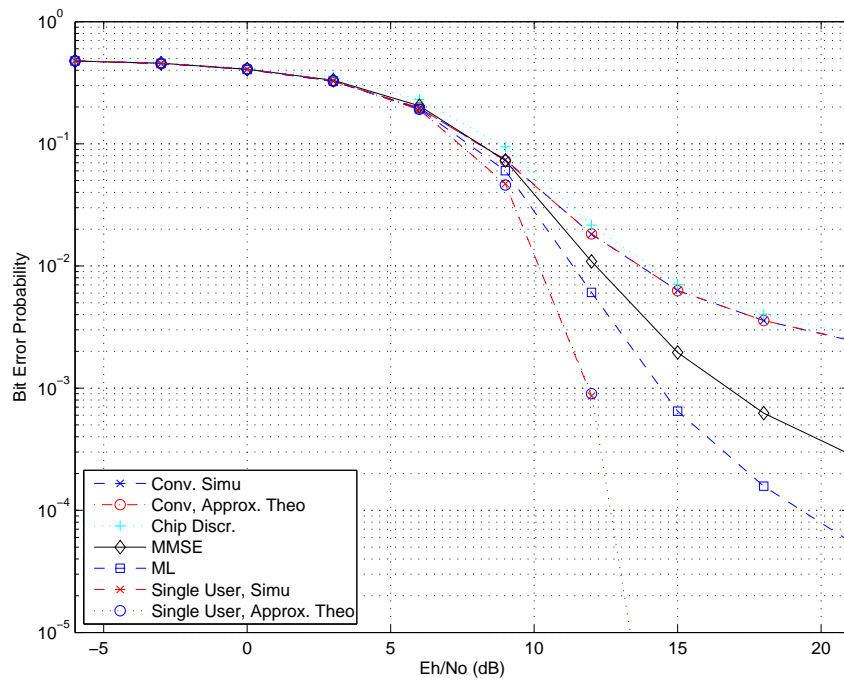

Figure 4.12: BEP versus E_h/N_0 for a 2-user system for CM2 with $N_f = 4$, $N_c = 250$ and $E_k = 1$ for $k = 1, 2$.
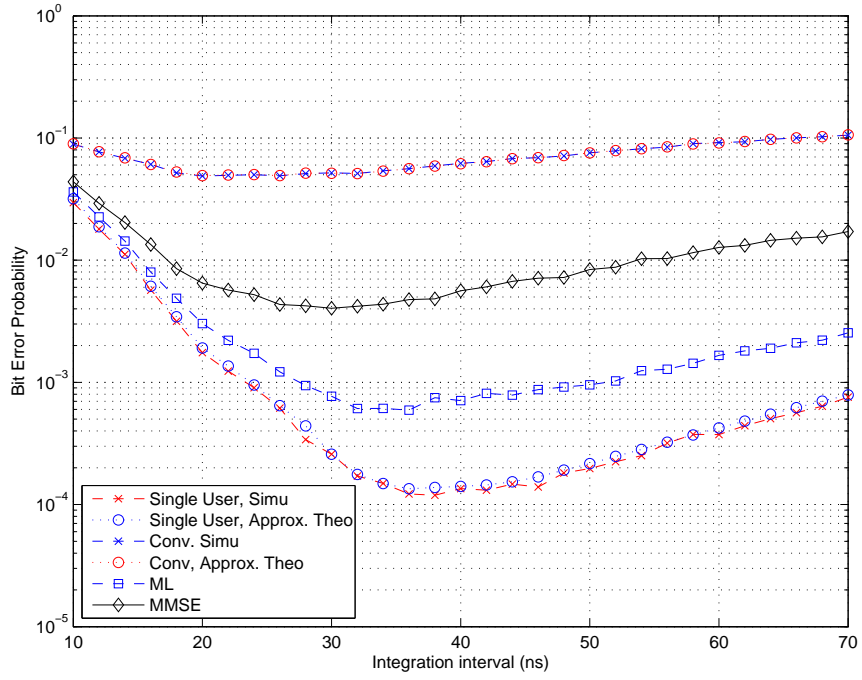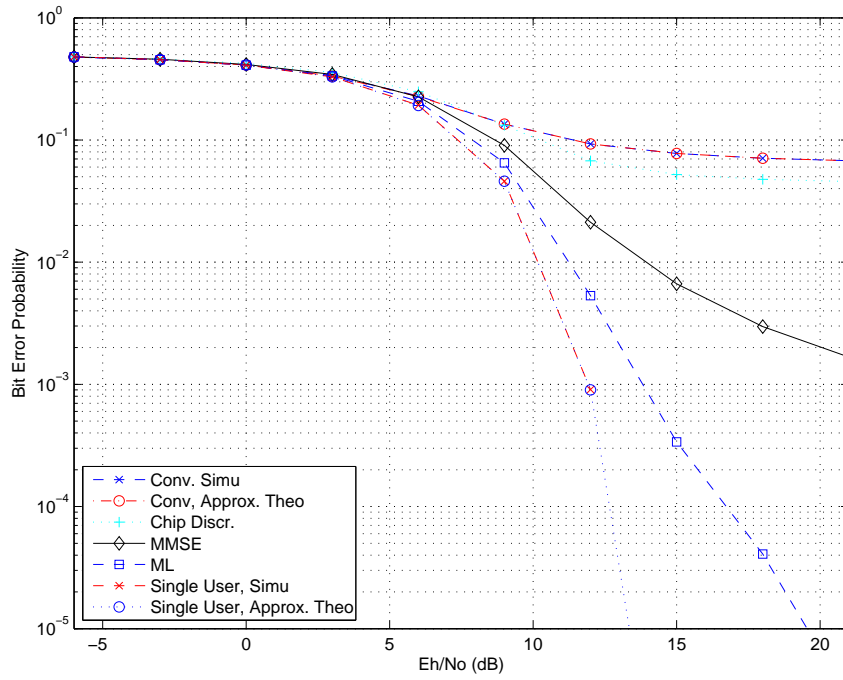
Figure 4.13: BEP versus E_h/N_0 for a 2-user system for CM2 with $N_f = 4$, $N_c = 250$, $E_1 = 1$ and $E_2 = 2$.

Figure 4.14: BEP versus E_h/N_0 for a 2-user system for CM3 with $N_f = 4$, $N_c = 250$ and $E_k = 1$ for $k = 1, 2$.
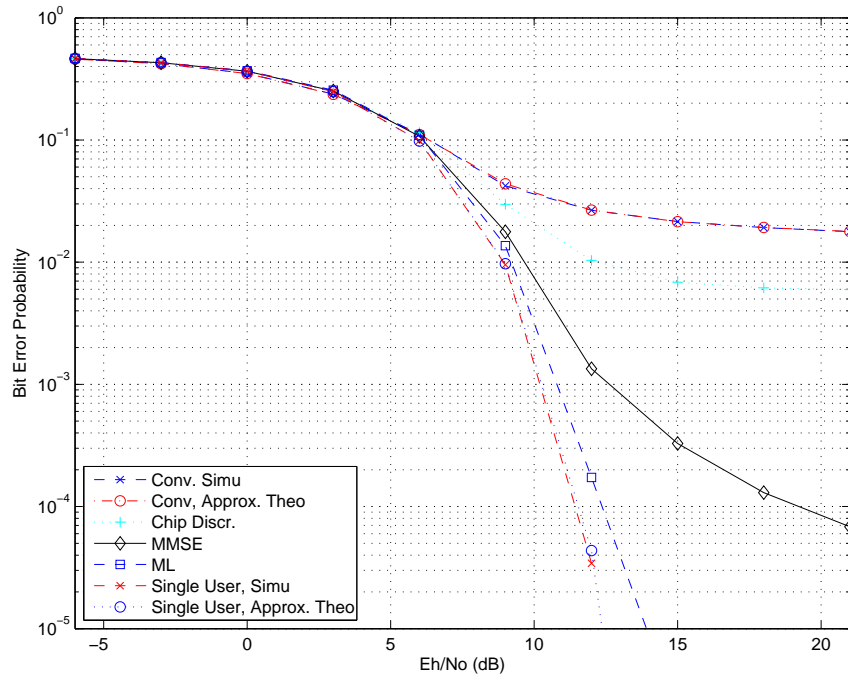
Figure 4.15: BEP versus E_h/N_0 for a 2-user system for CM3 with $N_f = 4$, $N_c = 250$, $E_1 = 1$ and $E_2 = 2$.
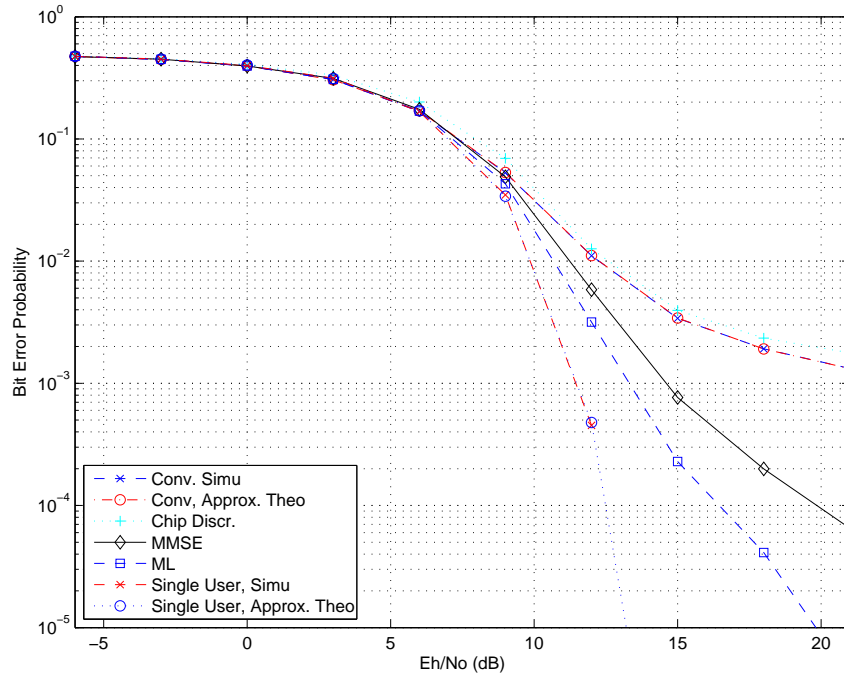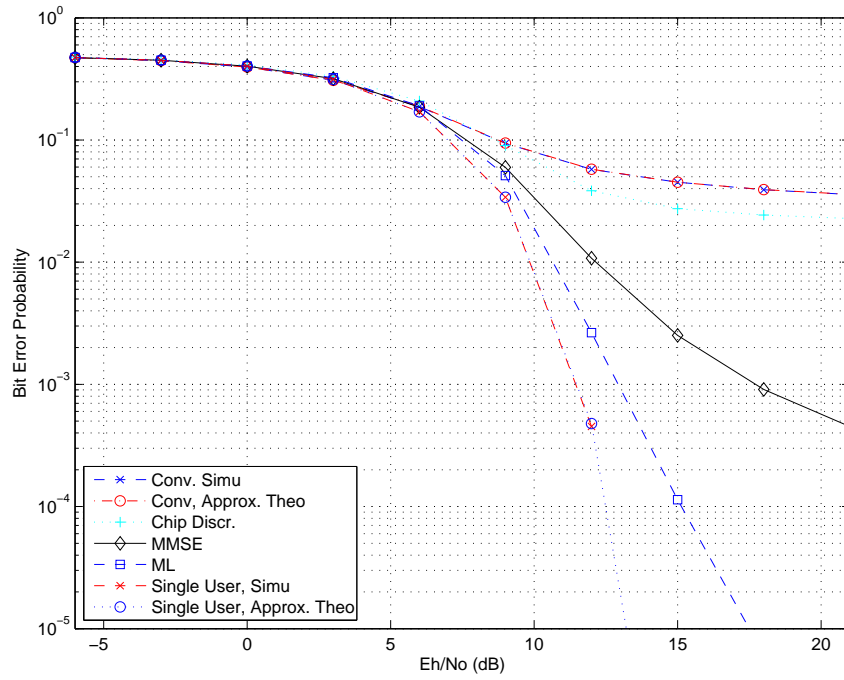

Figure 4.16: BEP versus E_h/N_0 for a 2-user system for CM4 with $N_f = 4$, $N_c = 250$ and $E_k = 1$ for $k = 1, 2$.
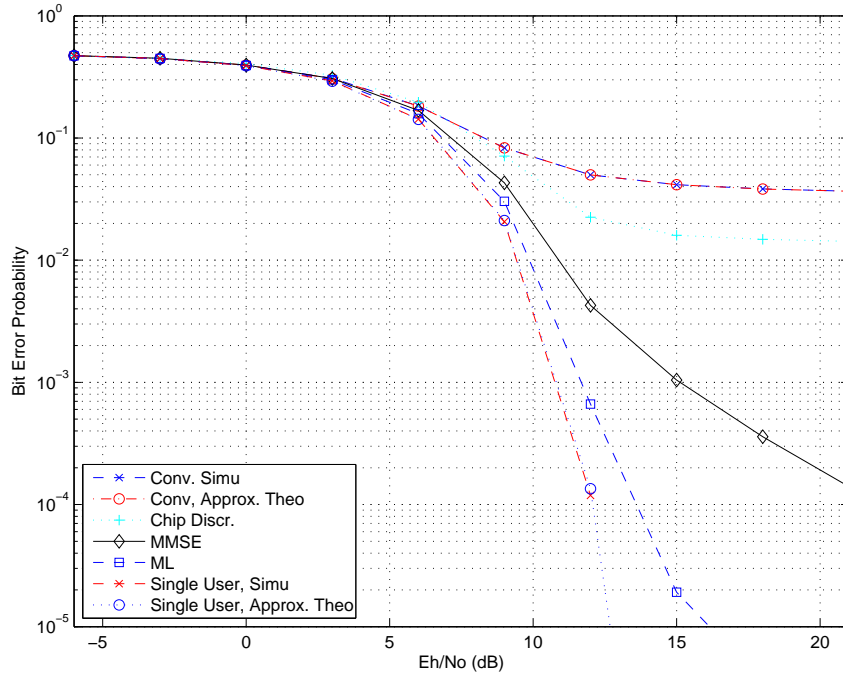
Figure 4.17: BEP versus E_h/N_0 for a 2-user system for CM4 with $N_f = 4$, $N_c = 250$, $E_1 = 1$ and $E_2 = 2$.

Figures 4.10–4.17 plot the BEP for the previously discussed system parameters. The BEPs are obtained as a function of the signal-to-noise ratio (SNR) defined in terms of E_h/N_o, where E_h is the energy of $h(t)$ given by

$$E_h = \int_\Gamma h^2(t)dt \; , \tag{4.3}$$

with $h(t) = \sqrt{\frac{E_1}{2N_f}}\, \tilde{w}(t)$ and $\tilde{w}(t)$ being the channel response to the unit energy pulse $w(t)$ given in Figure 4.1. Note that, in order to make a fair comparison between different receivers, the optimal integration intervals in Tables 4.2 and 4.3 are used.

From the plots, it is observed that increasing the energy of the interfering user, E_2, degrades the performances of the conventional receiver and the linear MMSE receiver, as expected. However, the performance of the ML detector improves for the higher energy of the interfering user. This can be explained by

the fact that ML detector assumes the knowledge of the parameters including the symbol energy of the interfering user. Thus, increasing the energy of the interfering user may provide improved detection performance. The chip discriminator also performs better in the second scenario. This is an expected result, since discarding the colliding pulses with higher interfering energies provides improved performance. Note that, for large value of M, the PDF of the chi-square distribution cannot be computed. Instead, the PDF given in (3.28) is used. Note also that, among all the receivers, the ML receiver performs the closest to the single user case. However, it assumes the most prior knowledge and has a more complex structure than the other receivers.

The theoretical results of the single user case are the same in both scenarios as expected and match with the simulation results perfectly for CM1 and CM2. In channel models CM3 and CM4, the integration interval Γ is taken to be shorter, which results in a small value of M ($M = 2B|\Gamma| + 1$). Hence, the assumption of large $MN_f/2$ is not satisfied well in those cases. As observed from the figures, there is a good agreement between the theoretical and the simulation results for the two-user case.

Figures 4.18–4.21 plot the BEP versus the integration interval $|\Gamma|$ for a three-user system for channel models CM1, CM2, CM3, and CM4, respectively. All the users have equal symbol energies ($E_k = 1$ for $k = 1, 2, 3$).

Figure 4.18: BEP versus $|\Gamma|$ for a 3-user system for CM1 with $N_f = 4$, $N_c = 250$ and $E_k = 1$ for $k = 1, 2, 3$.

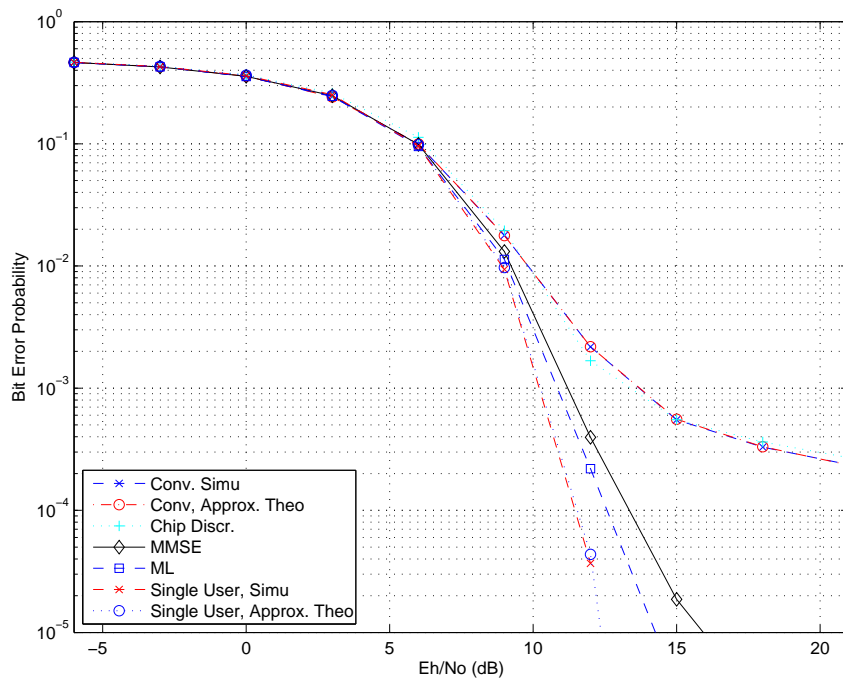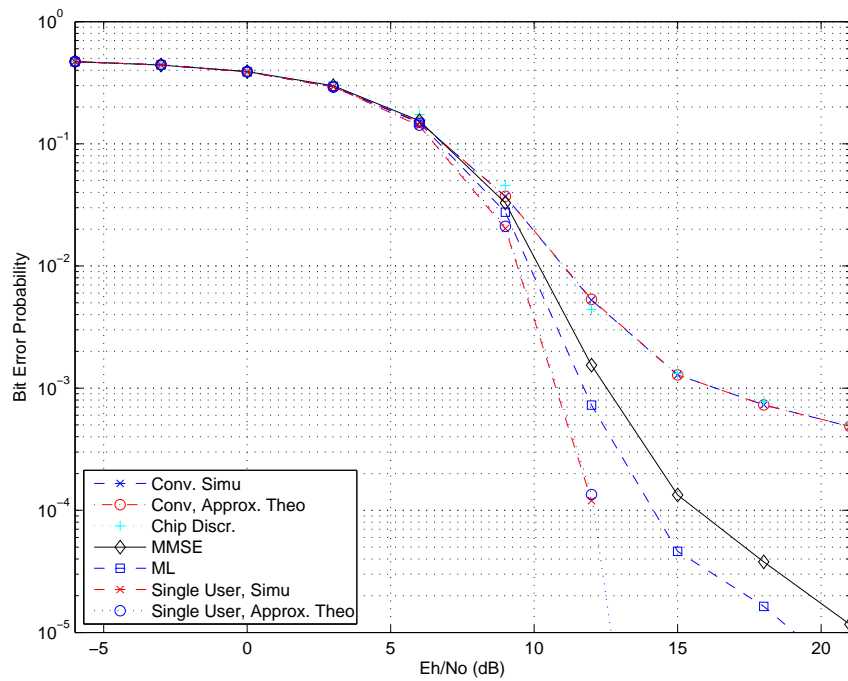Figure 4.19: BEP versus $|\Gamma|$ for a 3-user system for CM2 with $N_f = 4$, $N_c = 250$ and $E_k = 1$ for $k = 1, 2, 3$.
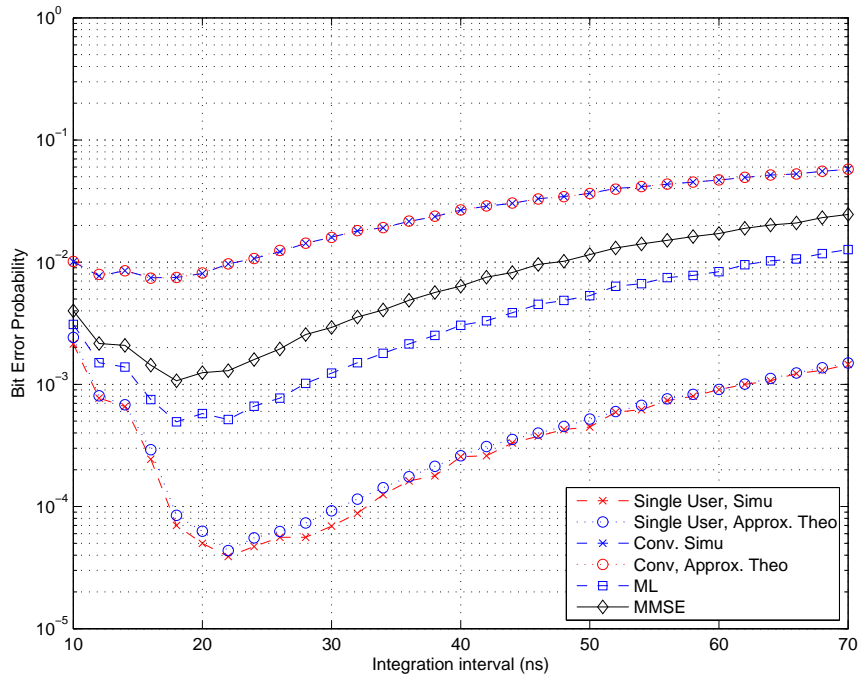
Figure 4.20: BEP versus $|\Gamma|$ for a 3-user system for CM3 with $N_f = 4$, $N_c = 250$ and $E_k = 1$ for $k = 1, 2, 3$.
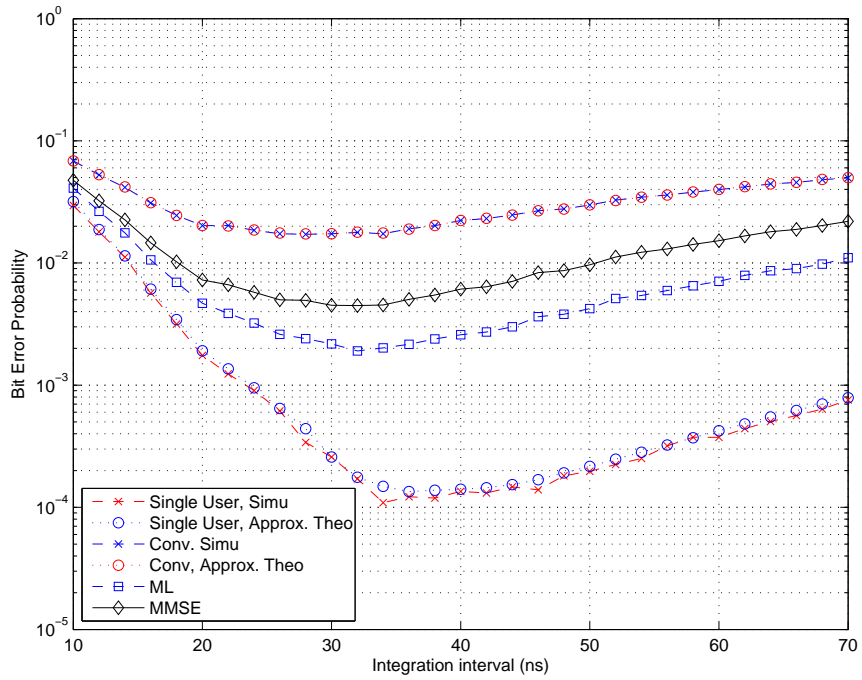
Figure 4.21: BEP versus $|\Gamma|$ for a 3-user system for CM4 with $N_f = 4$, $N_c = 250$ and $E_k = 1$ for $k = 1, 2, 3$.

The integration intervals for the minimum probability of error are given in Table 4.4. From the table, it is observed that the performances of receivers are highly dependent on the integration interval and the optimal value of the integration duration varies from receiver to receiver as in the previous scenarios.

Table 4.4: Optimal integration intervals for CM1, CM2, CM3 and CM4 channel models in a 3-user system ($E_k = 1$ for $k = 1, 2, 3$) with 12 dB SNR value. All the quantities are in the unit of nanosecond (ns).

Channel Model	Single User, Simu.	Single User, Theo.	Conv. Rec., Simu.	Conv. Rec., Theo.	MMSE Receiver	ML Detector
CM1	48	48	20	20	26	34
CM2	54	54	36	36	38	38
CM3	22	22	16	16	18	18
CM4	36	36	28	28	30	32
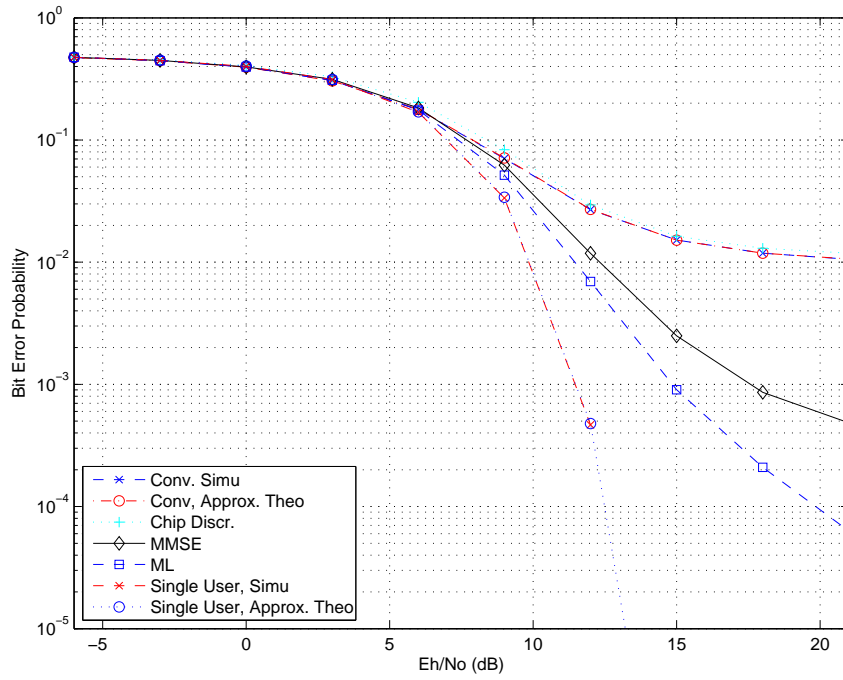
Figure 4.22: BEP versus E_h/N_0 for a 3-user system for CM1 with $N_f = 4$, $N_c = 250$ and $E_k = 1$ for $k = 1, 2, 3$.
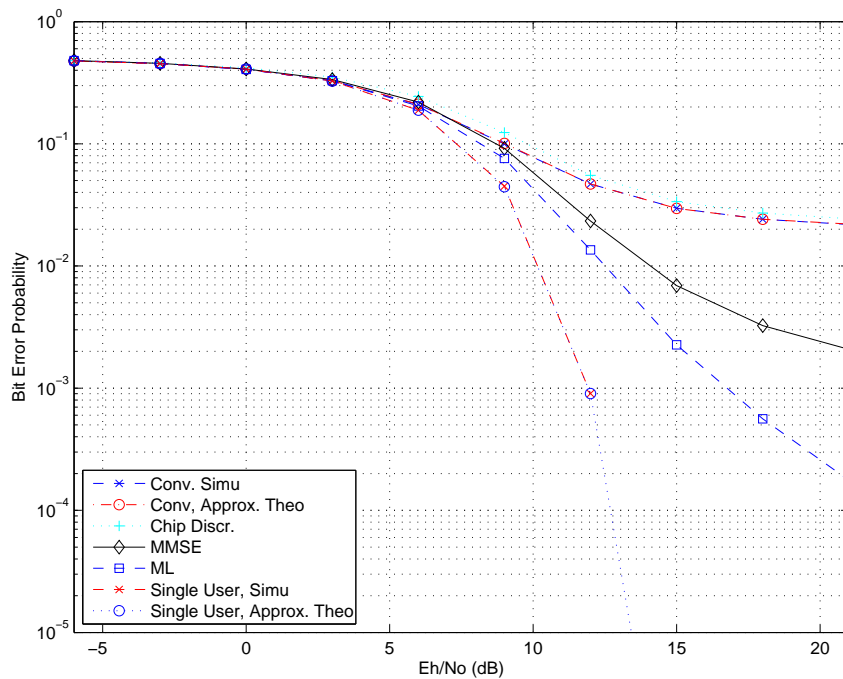
Figure 4.23: BEP versus E_h/N_0 for a 3-user system for CM2 with $N_f = 4$, $N_c = 250$ and $E_k = 1$ for $k = 1, 2, 3$.

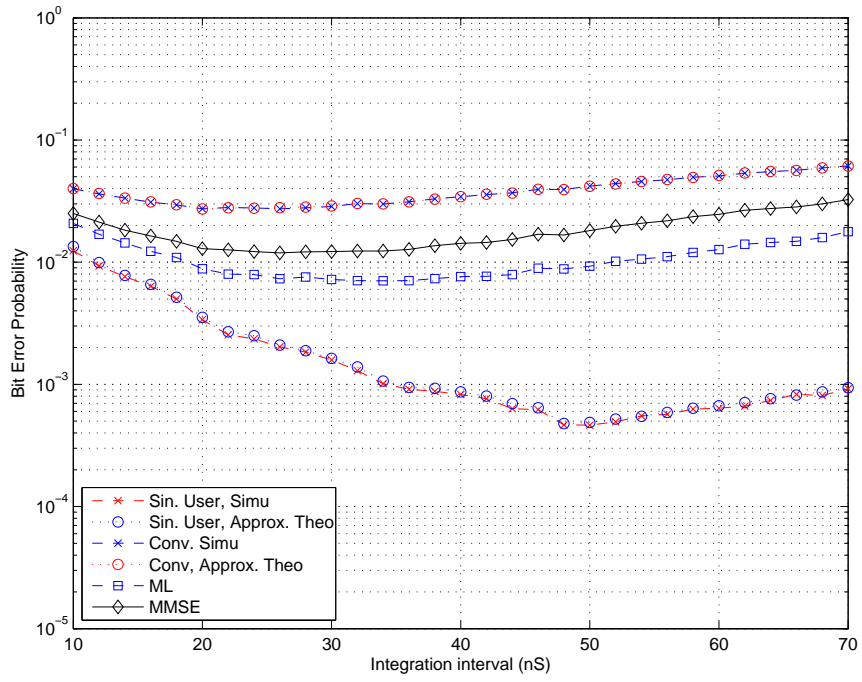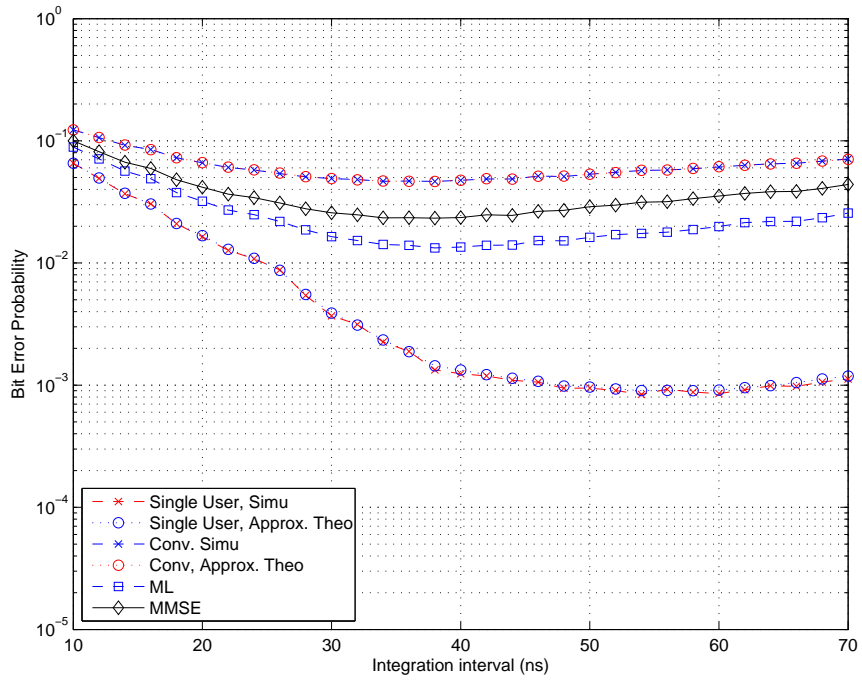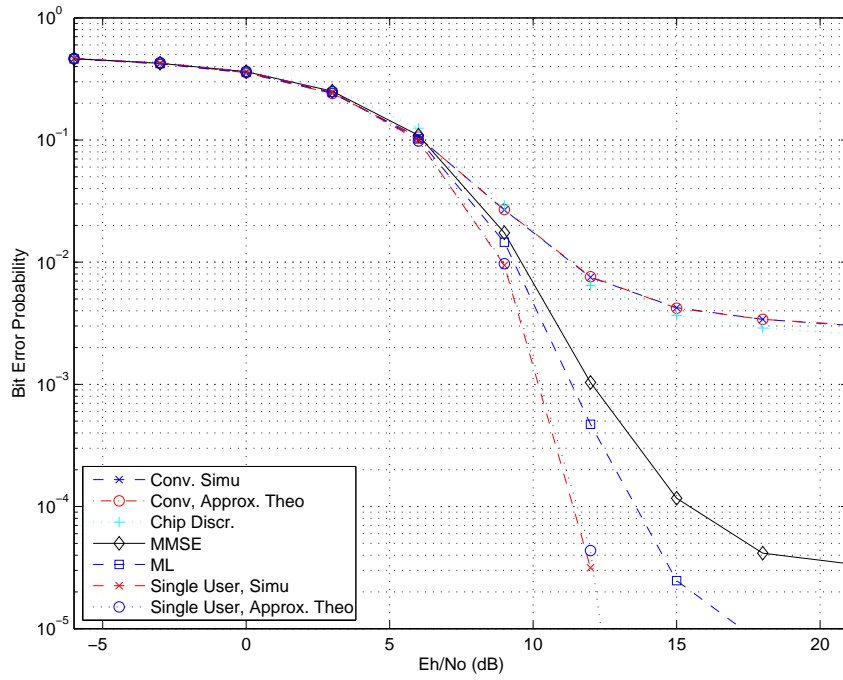Figure 4.24: BEP versus E_h/N_0 for a 3-user system for CM3 with $N_f = 4$, $N_c = 250$ and $E_k = 1$ for $k = 1, 2, 3$.
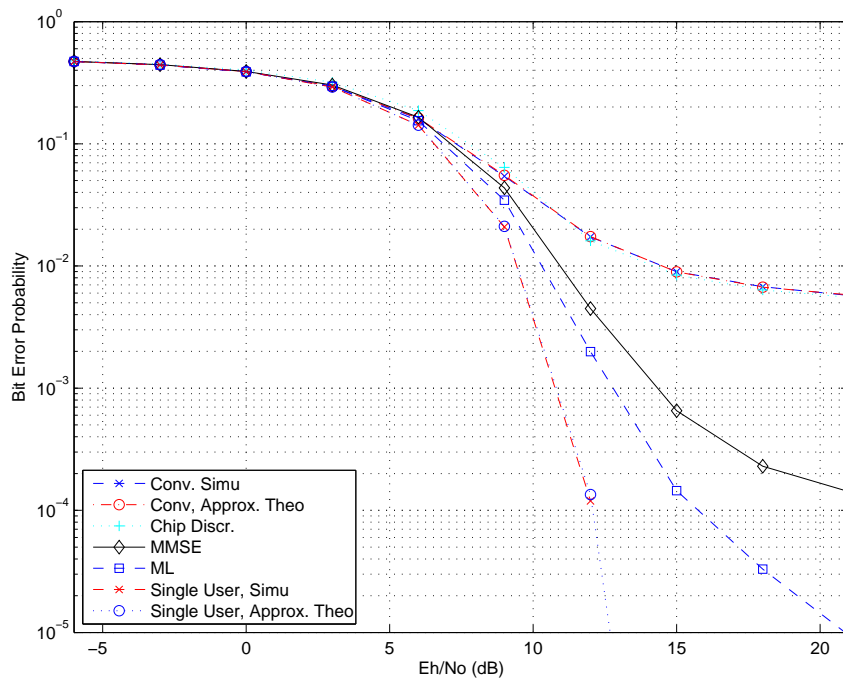
Figure 4.25: BEP versus E_h/N_0 for a 3-user system for CM4 with $N_f = 4$, $N_c = 250$ and $E_k = 1$ for $k = 1, 2, 3$.

Figures 4.22–4.25 plot the BEP versus E_h/N_o, where E_h is the energy of $h(t)$ as given in (4.3). Note that, in order to make a fair comparison between different receivers, the optimal integration intervals in Table 4.4 are used. From the plots, it is observed that the simulation results match well with the theoretical calculations for the conventional receivers in the three-user scenario. Compared to the two-user scenario, the performance of all the receivers degrades. Also, the chip discriminator performs very closely to the conventional receiver.

Chapter 5

Conclusions

In this thesis, the performance of CM-TR systems has been analyzed and the probability of error expressions have been obtained. For the single user case, a closed form expression of the exact error probability has been derived. For the multiuser case, a closed form expression based on the Gaussian approximation is presented. Simulation results have matched closely with the theoretical analysis for realistic channel models.

Besides the conventional receiver employed in CM-TR systems, some optimal and suboptimal receivers have been proposed. First, low-complexity receivers such as the blinking receiver (BR) and the chip discriminator have been presented. In the former case, the knowledge of TH sequences is required and the decision is made based on the uncorrupted pulses of the user of interest. In the latter case, the symbol energies of the users are needed together with the TH sequences, and two threshold levels are set for both the TH sequences and the symbol energies of the users. Due to the highly dispersive nature of UWB channels and the related system parameters, these receivers are inefficient and perform poorly in many cases. Then, the linear minimum mean-squared error (MMSE) receiver has been derived, and its performance has been analyzed. Finally, the

optimal maximum-likelihood (ML) detector has been derived, which has higher computational complexity and more strict requirements than the other receivers. Simulation results have shown that the linear MMSE receiver is the best among the considered suboptimal receivers.

APPENDIX A

Chi-Square Distribution

Let $X_1, \ldots, X_i, \ldots, X_k$ be independent Gaussian distributed random variables with means μ_i and variances σ_i^2. Then, the random variable

$$X = \sum_{i=1}^{k} \left(\frac{X_i}{\sigma_i} \right)^2 \tag{A.1}$$

is distributed as a chi-square random variable with k degrees of freedom and parameter λ given as

$$\lambda = \sum_{i=1}^{k} \left(\frac{\mu_i}{\sigma_i} \right)^2 . \tag{A.2}$$

For random variable X defined in (A.1), the probability density function (PDF) and the cumulative distribution function (CDF) can be written respectively as [33]

$$p(x) = \frac{1}{2} e^{-(x+\lambda)/2} \left(\frac{x}{\lambda} \right)^{k/4-1/2} I_{k/2-1}(\sqrt{kx} \, ,) \tag{A.3}$$

$$F(x) = \sum_{j=0}^{\infty} e^{-\lambda/2} \frac{(\lambda/2)^j}{j!} \frac{\gamma(j+k/2, x/2)}{\Gamma(j+k/2)} , \tag{A.4}$$

where $I_v(z)$ is the vth order modified Bessel function of the first kind, $\Gamma(n) = (n-1)!$ is the gamma function and $\gamma(k, z)$ is the lower incomplete gamma function.

For the conventional receiver, the energy obtained from the jth frame can be expressed as

$$y_j = \int_{jT_f}^{(j+1)T_f} [\tilde{w}(t) + n(t)]^2 \, dt \, , \quad j = 0, \ldots, N_f - 1 \, , \tag{A.5}$$

where $\tilde{w}(t)$ is the deterministic received pulse and $n(t)$ is zero mean Gaussian noise with a flat spectral density of σ^2 over the system bandwidth. Thus, y_j can be shown to be distributed as a central chi-square random variable [25]. In other words, y_j can be denoted as $\chi_M^2(\theta)$, where M is the degrees of freedom obtained as $2BT_f + 1$ and θ is the signal energy (in the absence of noise), which can be obtained as $\int_{jT_f}^{(j+1)T_f} |\tilde{w}(t)|^2 \, dt$.

For large M, the filtered noise and data pulse over the integration interval of duration T_f can be written as [25]

$$\sum_{i=1}^{M} n_i \phi_i(t) \quad \text{and} \quad \sum_{i=1}^{M} \mu_i \phi_i(t) \, , \tag{A.6}$$

where ϕ_i's are orthonormal functions over the integration interval and n_i's are zero mean independent Gaussian random variables with variances σ^2. Thus, from (A.5), random variable Y can be defined as

$$Y = \int_{jT_f}^{(j+1)T_f} \left(\sum_{i=1}^{M} (\mu_i + n_i) \phi_i(t) \right)^2 dt = \sum_{i=1}^{M} (\mu_i + n_i)^2 \, . \tag{A.7}$$

Thus, from (A.1), the expression

$$Y = \sigma^2 X \tag{A.8}$$

can be obtained. In a similar way, θ (the signal energy in the absence of noise) can be written as

$$\theta = \int_{jT_f}^{(j+1)T_f} \left(\sum_{i=1}^{M} \mu_i \phi_i(t) \right)^2 dt = \sum_{i=1}^{M} \mu_i^2 = \sigma^2 \lambda \, , \tag{A.9}$$

where λ is given in (A.2). Therefore, from (A.3) and (A.4), the PDF and the CDF of random variable Y can be expressed as

$$p(y) = \frac{1}{2\sigma^2} e^{\frac{-(y+\theta)}{2\sigma^2}} \left(\frac{y}{\theta}\right)^{\frac{M}{4}-\frac{1}{2}} I_{M/2-1}\left(\frac{\sqrt{\theta y}}{\sigma^2}\right) , \tag{A.10}$$

$$F(y) = \sum_{j=0}^{\infty} e^{-\theta/2\sigma^2} \frac{(\theta/2\sigma^2)^j}{j!} \frac{\gamma(j+\theta/2\sigma^2, y/2\sigma^2)}{\Gamma(j+\theta/2\sigma^2)} . \tag{A.11}$$

Note that if there is no pulse in frame j or if pulses from different users cancel each other, than the energy sample y_j can be shown to be distributed as

$$y_j = \int_{jT_f}^{(j+1)T_f} n^2(t)dt = \chi_M(0) . \tag{A.12}$$

For large values of M, the filtered noise $n(t)$ can be written as

$$\sum_{i=1}^{M} n_i \phi_i(t) , \tag{A.13}$$

where ϕ_i's are orthonormal functions over the integration interval T_f and n_i's are zero mean Gaussian random variables with variance σ^2. Then, random variable Y can be defined as

$$Y = \int_{jT_f}^{(j+1)T_f} \left(\sum_{i=1}^{M} n_i \phi_i(t)\right)^2 dt = \sum_{i=1}^{M} n_i^2 . \tag{A.14}$$

Therefore, the PDF and the CDF of random variable Y can be obtained as

$$p(y) = \frac{y^{M/2-1} e^{-y/2\sigma^2}}{\sigma^M 2^{M/2} \Gamma(M/2)} , \tag{A.15}$$

$$F(y) = \frac{\gamma(k/2, y/2\sigma^2)}{\Gamma(k/2)} . \tag{A.16}$$

Note that, in the calculations above, the integration interval is taken as T_f. If the TH sequences are known, then it can be taken to be smaller than the frame interval T_f in order to collect less noise and to increase the signal-to-noise ratio (SNR) [34]. In that case, the degrees of freedom becomes $M = 2B|\Gamma_j|+1$, where Γ_j is the integration interval.

APPENDIX B

Proof of Lemmas 2.1 and 2.2

Let Y_j denote the random variable for the energy sample obtained from the jth frame. Then,

$$Y_j = \int_{jT_f}^{(j+1)T_f} r^2(t)dt \qquad j = 0, \ldots, N_f - 1 \; , \tag{B.1}$$

where $r(t)$ is the received signal and T_f is the frame interval. For frames with no pulses, Y_j can be defined from (A.14) as

$$Y_j = \sum_{i=1}^{M} n_i^2 \; , \tag{B.2}$$

where n_i's zero mean independent Gaussian random variables with variance σ^2. Then,

$$E\{Y_j\} = \sum_{i=1}^{M} E\{n_i^2\} \tag{B.3}$$

$$= \sigma^2 M$$

$$E\{Y_j^2\} = \sum_{i,k=1}^{M} E\{n_i^2 n_k^2\} \tag{B.4}$$

$$= \sum_{i=1}^{M} E\{n_i^4\} + \sum_{i \neq k=1}^{M} E\{n_i^2\} E\{n_k^2\}$$

$$= 3\sigma^4 M + (M^2 - M)\sigma^2 \sigma^2$$

$$= (M^2 + 2M)\sigma^4$$

$$Var(Y_j) = E\{Y_j^2\} - E^2\{Y_j\} \tag{B.5}$$

$$= 2M\sigma^4$$

Hence,

$$Y_j \sim \mathcal{N}\left(M\sigma^2,\ 2M\sigma^4\right)\ . \tag{B.6}$$

Note that, for $b^{(1)} = -1$, no pulses are transmitted in the frames indexed by S. It can be shown that the summation $D_1 = \sum_{j \in S} Y_j$ is also Gaussian distributed.

$$E\{D_1\} = \sum_{j=1}^{N_f/2} E\{Y_j\} \tag{B.7}$$

$$= \frac{\sigma^2 M N_f}{2}$$

$$Var(D_1) = \sum_{j=1}^{N_f/2} Var(Y_j) \tag{B.8}$$

$$= \sigma^4 M N_f$$

Thus,

$$D_1 \sim \mathcal{N}\left(\frac{\sigma^2 M N_f}{2}, \sigma^4 M N_f\right)\ . \tag{B.9}$$

If there is any data pulse in the jth frame,

$$Y_j = \int_{jT_f}^{(j+1)T_f} \left(\sum_{i=1}^{M} (\mu_i + n_i \phi_i(t))\right)^2 dt = \sum_{i=1}^{M} (\mu_i + n_i)^2\ , \tag{B.10}$$

55

where $\sum_{i=1}^{M} \mu_i^2 = \theta_j(\mathbf{b})$ is the energy obtained (in the absence of noise) from the jth frame for binary information bits $\mathbf{b}$. Thus,

$$E\{Y_j\} = M\sigma^2 + \theta_j(\mathbf{b}) \ . \tag{B.11}$$

If we define $X_i = (\mu_i + n_i)^2$, then

$$
\begin{aligned}
E\{Y_j^2\} &= \sum_{i,j=1}^{M} E\{X_i^2 X_j^2\} \\
&= \sum_{i=1}^{M} E\{X_i^4\} + \sum_{i \neq j=1}^{M} E\{X_i^2\} E\{X_j^2\} \\
&= \sum_{i=1}^{M} E\{X_i^4\} + \left[\sum_{i=1}^{M} E\{X_i^2\}\right]^2 - \sum_{i=1}^{M} \left[E\{X_i^2\}\right]^2
\end{aligned}
$$

$$\tag{B.12}$$

$$
\begin{aligned}
Var(Y_j) &= E\{Y_j^2\} - E^2\{Y_j\} \\
&= \sum_{i=1}^{M} E\{X_i^4\} - \sum_{i=1}^{M} \left[E\{X_i^2\}\right]^2 \\
&= \sum_{i=1}^{M} E\{(u_i + n_i)^4\} - \sum_{i=1}^{M} \left[E\{X_i^2\}\right]^2, \qquad n_i \sim (0, \sigma^2) \\
&= \sum_{i=1}^{M} E\{n_i^4 + 4n_i^3 u_i + 6n_i^2 u_i^2 + 4n_i u_i^3 + u_i^4\} - \sum_{i=1}^{M} \left[E\{X_i^2\}\right]^2 \\
&= \sum_{i=1}^{M} (3\sigma^4 + 6\sigma^2 u_i^2 + u_i^4) - \sum_{i=1}^{M} (\sigma^2 + u_i^2)^2 \\
&= 2\sigma^4 M + 4\sigma^2 \sum_{i=1}^{M} u_i^2 \\
&= 2\sigma^4 M + 4\sigma^2 \theta_j(\mathbf{b}) \tag{B.13}
\end{aligned}
$$

The summation $D_2 = \sum_{j \in \bar{S}} Y_j$ has the following parameters:

$$
\begin{aligned}
E\{D_2\} &= \sum_{j \in \bar{S}} E\{Y_j\} \tag{B.14} \\
&= \frac{\sigma^2 M N_f}{2} + \sum_{j \in \bar{S}} \theta_j(\mathbf{b}) \ .
\end{aligned}
$$

$$Var(D_2) = \sum_{j \in \bar{S}} Var(Y_j) \tag{B.15}$$

$$= \sigma^4 M N_f + 4\sigma^2 \sum_{j \in \bar{S}} \theta_j(\mathbf{b}) \ . $$

Thus, D_2 is Gaussian distributed as

$$D_2 \sim \mathcal{N} \left(\frac{\sigma^2 M N_f}{2} + \sum_{j \in \bar{S}} \theta_j(\mathbf{b}), \ \sigma^4 M N_f + 4\sigma^2 \sum_{j \in \bar{S}} \theta_j(\mathbf{b}) \right) \tag{B.16}$$

Similarly, D_1 is distributed as

$$D_1 \sim \mathcal{N} \left(\frac{\sigma^2 M N_f}{2} + \sum_{j \in S} \theta_j(\mathbf{b}), \ \sigma^4 M N_f + 4\sigma^2 \sum_{j \in S} \theta_j(\mathbf{b}) \right) \tag{B.17}$$

Since D_1 and D_2 are independent Gaussian random variables, their difference is also Gaussian distributed as

$$D = (D_1 - D_2) \sim \mathcal{N} \left(\sum_{j \in S} \theta_j(\mathbf{b}) - \sum_{j \in \bar{S}} \theta_j(\mathbf{b}), \ 2\sigma^4 M N_f + 4\sigma^2 \sum_{j=0}^{N_f - 1} \theta_j(\mathbf{b}) \right) \tag{B.18}$$

Assume that the only user in the system is user 1. Then, equations above reduce to

$$\mathbf{b} = b^{(1)} = -1 \ \Rightarrow \ D_1 \sim \mathcal{N} \left(\frac{\sigma^2 M N_f}{2}, \ \sigma^4 M N_f \right) \tag{B.19}$$

$$\Rightarrow \ D_2 \sim \mathcal{N} \left(\frac{\sigma^2 M N_f}{2} + \frac{\theta N_f}{2}, \ \sigma^4 M N_f + 2\sigma^2 \theta N_f \right) \tag{B.20}$$

$$\Rightarrow \ D \sim \mathcal{N} \left(-\frac{\theta N_f}{2}, \ 2\sigma^4 M N_f + 2\sigma^2 \theta N_f \right) \ . \tag{B.21}$$

APPENDIX C

Proof of Lemma 3.1

In Chapter 3, n_j is defined as

$$n_j = \sqrt{\frac{2E_1}{N_f}} a_j^{(1)} \int_{\Gamma_j} \tilde{w}(t - jT_f - c_j^{(1)}T_c)[r_I(t) + n(t)]dt + \int_{\Gamma_j} [r_I(t) + n(t)]^2 dt .$$

(C.1)

Taking the expectation of both sides,

$$E\{n_j\} = \sqrt{\frac{2E_1}{N_f}} a_j^{(1)} \int_{\Gamma_j} \tilde{w}\left(t - jT_f - c_j^{(1)}T_c\right) \sum_{k=2}^{K} \sqrt{\frac{E_k}{2N_f}} a_j^{(k)} E\{1 + b^{(k)}\tilde{d}_j^{(k)}\}$$

$$\times \tilde{w}\left(t - jT_f - c_j^{(k)}T_c\right) dt + \int_{\Gamma_j} E\left\{[r_I(t) + n(t)]^2\right\} dt .$$

(C.2)

Assume $b^{(k)} \in \{-1, +1\}$ with equal probability and define

$$R_{\tilde{w}}^j((c_j^{(1)} - c_j^{(k)})T_c) = \int_{\Gamma_j} \tilde{w}\left(t - jT_f - c_j^{(1)}T_c\right) \tilde{w}\left(t - jT_f - c_j^{(k)}T_c\right) dt .$$

(C.3)

Then, (C.2) can be written as

$$E\{n_j\} = \sqrt{\frac{2E_1}{N_f}} a_j^{(1)} \sum_{k=2}^{K} \sqrt{\frac{E_k}{2N_f}} a_j^{(k)} R_{\tilde{w}}^j((c_j^{(1)} - c_j^{(k)})T_c)$$

$$+ \int_{\Gamma_j} E\left\{r_I(t)^2\right\} dt + \int_{\Gamma_j} E\left\{n(t)^2\right\} dt .$$

(C.4)

Note that in the equation above, $n(t)$ is zero mean Gaussian noise and

$$\int_{\Gamma_j} E\left\{r_I(t)n(t)\right\} dt = \int_{\Gamma_j} E\left\{r_I(t)\right\} E\left\{n(t)\right\} dt = 0 . \tag{C.5}$$

Note also that, since the received signal passes through a low-pass filter with bandwidth B, we have colored noise. Thus, in (C.4),

$$\int_{\Gamma_j} E\left\{n(t)^2\right\} dt = |\Gamma_j|2B\sigma^2 , \tag{C.6}$$

where $|\Gamma_j|$ is the duration of the integration interval for frame j.

From (3.6) and (3.7),

$$\left[r_I^j(t)\right]^2 = \sum_{k_1=2}^{K}\sum_{k_2=2}^{K}\frac{\sqrt{E_{k_1}E_{k_2}}}{2N_f}a_j^{(k_1)}a_j^{(k_2)}\left(1 + b^{(k_1)}\tilde{d}_j^{(k_1)}\right)\left(1 + b^{(k_2)}\tilde{d}_j^{(k_2)}\right)$$
$$\times \tilde{w}\left(t - jT_f - c_j^{(k_1)}T_c\right)\tilde{w}\left(t - jT_f - c_j^{(k_2)}T_c\right) . \tag{C.7}$$

Taking the expectation and integrating the both sides in the equation above, we obtain

$$\int_{\Gamma_j} E\left\{\left[r_I^j(t)\right]^2\right\} dt =$$
$$\sum_{k_1=2}^{K}\sum_{k_2=2}^{K}\frac{\sqrt{E_{k_1}E_{k_2}}}{2N_f}a_j^{(k_1)}a_j^{(k_2)}\left(1 + \delta\left[k_1 - k_2\right]\right)R_{\tilde{w}}^j((c_j^{(k_1)} - c_j^{(k_2)})T_c) \tag{C.8}$$

Note that the equation above follows from (C.3) and the fact that $b^{(k)} \in \{-1, +1\}$ with equal probability. Thus, from (C.6) and (C.8),

$$E\{n_j\} = \sum_{k=2}^{K}\frac{\sqrt{E_1 E_k}}{N_f}a_j^{(1)}a_j^{(k)}R_{\tilde{w}}^j((c_j^{(1)} - c_j^{(k)})T_c) + \sum_{k_1=2}^{K}\sum_{k_2=2}^{K}\frac{\sqrt{E_{k_1}E_{k_2}}}{2N_f}a_j^{(k_1)}a_j^{(k_2)}$$
$$\times (1 + \delta\left[k_1 - k_2\right])R_{\tilde{w}}^j((c_j^{(k_1)} - c_j^{(k_2)})T_c) + |\Gamma_j|2B\sigma^2 . \tag{C.9}$$

The polarity randomization codes $a_j^{(2)}, \ldots, a_j^{(k)}$ are assumed to be i.i.d. random variables that take values $\{-1, +1\}$ with equal probability. Then,

$$E\left\{n_j\right\} = \sum_{k=2}^{K}\frac{E_k}{N_f}\chi_{j,k} + |\Gamma_j|2B\sigma^2 , \tag{C.10}$$

59

where

$$\chi_{j,k} = \int_{\Gamma_j} \left[\tilde{w} \left(t - jT_f - c_j^{(k)} T_c \right) \right]^2 dt \ .$$

(C.11)

60

APPENDIX D

Proof of Lemma 3.2

From (C.1), the term $n_j n_l$ can be written as

$$n_j n_l = \frac{2E_1}{N_f} a_j^{(1)} a_l^{(1)} C_1 + \sqrt{\frac{2E_1}{N_f}} a_j^{(1)} C_2 + \sqrt{\frac{2E_1}{N_f}} a_l^{(1)} C_3 + C_4 , \qquad (D.1)$$

where

$$C_1 = \int\limits_{\Gamma_j} \int\limits_{\Gamma_l} \tilde{w}\left(t_1 - jT_f - c_j^{(1)}T_c\right) \tilde{w}\left(t_2 - lT_f - c_l^{(1)}T_c\right) [r_I(t_1) + n(t_1)] \qquad (D.2)$$

$$\times \, [r_I(t_2) + n(t_2)] \, dt_2 dt_1$$

$$C_2 = \int\limits_{\Gamma_j} \int\limits_{\Gamma_l} \tilde{w}\left(t_1 - jT_f - c_j^{(1)}T_c\right) [r_I(t_1) + n(t_1)] \, [r_I(t_2) + n(t_2)]^2 \, dt_2 dt_1 \qquad (D.3)$$

$$C_3 = \int\limits_{\Gamma_j} \int\limits_{\Gamma_l} \tilde{w}\left(t_2 - lT_f - c_l^{(1)}T_c\right) [r_I(t_2) + n(t_2)] \, [r_I(t_1) + n(t_1)]^2 \, dt_2 dt_1 \qquad (D.4)$$

$$C_4 = \int\limits_{\Gamma_j} \int\limits_{\Gamma_l} [r_I(t_1) + n(t_1)]^2 \, [r_I(t_2) + n(t_2)]^2 \, dt_2 dt_1 . \qquad (D.5)$$

In (D.2), taking the expectation of both sides,

$$E\{C_1\} = \int\limits_{\Gamma_j} \int\limits_{\Gamma_l} \tilde{w}\left(t_1 - jT_f - c_j^{(1)}T_c\right) \tilde{w}\left(t_2 - lT_f - c_l^{(1)}T_c\right) \qquad (D.6)$$

$$\times \, (E\{r_I(t_1)r_I(t_2)\} + R_N(t_1 - t_2)) \, dt_2 dt_1 .$$

The equation above follows from (C.5) and the fact

$$E\{n(t_1)n(t_2)\} = R_N(t_1 - t_2) . \qquad (D.7)$$

From (3.7) and assuming that $b^{(k)} \in \{-1, +1\}$ with equal probability,

$$
\begin{aligned}
E\left\{r_I(t_1)r_I(t_2)\right\} = \sum_{k_1=2}^{K} \sum_{k_2=2}^{K} \frac{\sqrt{E_{k_1}E_{k_2}}}{2N_f} a_j^{(k_1)} a_l^{(k_2)} \left(1 + \tilde{d}_j^{(k_1)} \tilde{d}_l^{(k_2)} \delta\left[k_1 - k_2\right]\right) \\
\times \tilde{w}\left(t_1 - jT_f - c_j^{(k_1)}T_c\right) \tilde{w}\left(t_2 - lT_f - c_l^{(k_2)}T_c\right)
\end{aligned}
\tag{D.8}
$$

Then, from (D.6) and (C.3),

$$
\begin{aligned}
E\left\{C_1\right\} = \sum_{k_1=2}^{K} \sum_{k_2=2}^{K} \frac{\sqrt{E_{k_1}E_{k_2}}}{2N_f} a_j^{(k_1)} a_l^{(k_2)} \left(1 + \tilde{d}_j^{(k_1)} \tilde{d}_l^{(k_2)} \delta\left[k_1 - k_2\right]\right) R_{\tilde{w}}^j((c_j^{(1)} - c_j^{(k_1)})T_c) \\
\times R_{\tilde{w}}^l((c_l^{(1)} - c_l^{(k_2)})T_c) + \int_{\Gamma_j} \int_{\Gamma_l} \tilde{w}\left(t_1 - jT_f - c_j^{(1)}T_c\right) \tilde{w}\left(t_2 - lT_f - c_l^{(1)}T_c\right) \\
\times R_N(t_1 - t_2)dt_2dt_1 \; .
\end{aligned}
\tag{D.9}
$$

Note that in the equation above, $R_N(t_1 - t_2) = 2\sigma^2 B\operatorname{sinc}(2B(t_1 - t_2))$; however, for large values of B, the approximation can be performed as

$$
R_N(t_1 - t_2) = \sigma^2 \delta(t_1 - t_2) \; .
\tag{D.10}
$$

Thus,

$$
\begin{aligned}
E\left\{C_1\right\} = \sum_{k_1=2}^{K} \sum_{k_2=2}^{K} \frac{\sqrt{E_{k_1}E_{k_2}}}{2N_f} a_j^{(k_1)} a_l^{(k_2)} \left(1 + \tilde{d}_j^{(k_1)} \tilde{d}_l^{(k_2)} \delta\left[k_1 - k_2\right]\right) \\
\times R_{\tilde{w}}^j((c_j^{(1)} - c_j^{(k_1)})T_c) R_{\tilde{w}}^l((c_l^{(1)} - c_l^{(k_2)})T_c) +
\begin{cases}
0, & j \neq l \\
\sigma^2 \gamma_j^{(1)}, & j = l
\end{cases}
\end{aligned}
\tag{D.11}
$$

where $\gamma_j^{(1)}$ is given in (3.9).

Also, from (D.3),

$$
\begin{aligned}
E\left\{C_2\right\} = \int_{\Gamma_j} \int_{\Gamma_l} \tilde{w}(t_1 - jT_f - c_j^{(1)}T_c) \\
\times E\left\{(r_I(t_1) + n(t_1))\left(r_I^2(t_2) + 2r_I(t_2)n(t_2) + n^2(t_2)\right)\right\} dt_2dt_1
\end{aligned}
\tag{D.12}
$$

Using the previous results,

$$
\begin{aligned}
E\left\{C_2\right\} = \int_{\Gamma_j} \int_{\Gamma_l} \tilde{w}(t_1 - jT_f - c_j^{(1)}T_c)_1 \left[E\{r_I(t_1)r_I^2(t_2)\} + 2B\sigma^2 E\{r_I(t_1)\} + \right. \\
\left. + 2E\{r_I(t_2)\}R_N(t_1 - t_2) + E\{n(t_1)n^2(t_2)\}\right] dt_2dt_1
\end{aligned}
\tag{D.13}
$$

62

Assuming that $b^{(k)} \in \{-1, +1\}$ with equal probability for user k,

$$E\{r_I(t_1)r_I^2(t_2)\} = \sum_{k_1=2}^{K} \sum_{k_2=2}^{K} \sum_{k_3=2}^{K} \frac{\sqrt{E_{k_1}E_{k_2}E_{k_3}}}{(2N_f)^{1.5}} a_j^{(k_1)} a_l^{(k_2)} a_l^{(k_3)} \tilde{e}\tilde{w}(t_1 - jT_f - c_j^{(k_1)}T_c)$$

$$\times \tilde{w}(t_2 - lT_f - c_l^{(k_2)}T_c)\tilde{w}(t_2 - lT_f - c_l^{(k_3)}T_c) , \qquad (D.14)$$

where

$$\tilde{e} = E\left\{(1 + b^{(k_1)}\tilde{d}_j^{(k_1)})(1 + b^{(k_2)}\tilde{d}_l^{(k_2)})(1 + b^{(k_3)}\tilde{d}_l^{(k_3)})\right\}$$

$$= \begin{cases} 1 & \text{if } k_1 \neq k_2 \neq k_3; \\ 1 + \tilde{d}_j^{(k_1)}\tilde{d}_l^{(k_1)} & \text{if } k_1 = k_2 \neq k_3 \\ & \text{or } k_1 = k_3 \neq k_2; \\ 2 & \text{if } k_2 = k_3 \neq 1; \\ 2 + \tilde{d}_j^{(k_1)}\tilde{d}_l^{(k_1)} & \text{if } k_1 = k_2 = k_3. \end{cases} \qquad (D.15)$$

Although $n(t)$ is colored noise, the following equality can be obtained after some approximation.

$$\int_{\Gamma_j} \int_{\Gamma_l} \tilde{w}(t_1 - jT_f - c_j^{(1)}T_c)E\{n(t_1)n^2(t_2)\}dt_2 dt_1 \approx 0 . \qquad (D.16)$$

From (3.7) and the results above, $E\{C_2\}$ can be expressed as

$$E\{C_2\} = \sum_{k_1=2}^{K} \sum_{k_2=2}^{K} \sum_{k_3=2}^{K} \frac{\sqrt{E_{k_1}E_{k_2}E_{k_3}}}{(2N_f)^{1.5}} a_j^{(k_1)} a_l^{(k_2)} a_l^{(k_3)} \tilde{e} R_{\tilde{w}}^j((c_j^{(1)} - c_j^{(k_1)})T_c)$$

$$\times R_{\tilde{w}}^l((c_l^{(k_2)} - c_l^{(k_3)})T_c) + 2B\sigma^2|\Gamma_l| \sum_{k=2}^{K} \sqrt{\frac{E_k}{2N_f}} a_j^{(k)} R_{\tilde{w}}^j((c_j^{(1)} - c_j^{(k)})T_c) +$$

$$+ 2 \begin{cases} 0 & , j \neq l \\ \sigma^2 \sum_{k=2}^{K} \sqrt{\frac{E_k}{2N_f}} a_j^{(k)} R_{\tilde{w}}^j((c_j^{(1)} - c_j^{(k)})T_c) & , j = l \end{cases} \qquad (D.17)$$

63

$E\{C_3\}$ can be found same as above if j and l are interchanged.

$$E\{C_3\} = \sum_{k_1=2}^{K} \sum_{k_2=2}^{K} \sum_{k_3=2}^{K} \frac{\sqrt{E_{k_1}E_{k_2}E_{k_3}}}{(2N_f)^{1.5}} a_l^{(k_1)} a_j^{(k_2)} a_j^{(k_3)} \tilde{e} R_{\tilde{w}}^l((c_l^{(1)} - c_l^{(k_1)})T_c)$$

$$\times R_{\tilde{w}}^j((c_j^{(k_2)} - c_j^{(k_3)})T_c) + 2B\sigma^2 |\Gamma_j| \sum_{k=2}^{K} \sqrt{\frac{E_k}{2N_f}} a_l^{(k)} R_{\tilde{w}}^l((c_l^{(1)} - c_l^{(k)})T_c) +$$

$$+ 2 \begin{cases} 0 & , j \neq l \\ \sigma^2 \sum\limits_{k=2}^{K} \sqrt{\frac{E_k}{2N_f}} a_l^{(k)} R_{\tilde{w}}^l((c_l^{(1)} - c_l^{(k)})T_c) & , j = l \end{cases} \tag{D.18}$$

In (D.5) taking the expectations of both sides and using the previous results,

$$E\{C_4\} = \int_{\Gamma_j} \int_{\Gamma_l} E\left\{(r_I(t_1) + n(t_1))^2 (r_I(t_2) + n(t_2))^2\right\} dt_2 dt_1$$

$$= \int_{\Gamma_j} \int_{\Gamma_l} \left[E\{r_I^2(t_1)r_I^2(t_2)\} + E\{r_I^2(t_1)\}2B\sigma^2 + 4E\{r_I(t_1)r_I(t_2)\}R_N(t_1 - t_2) + \right.$$

$$+ 2B\sigma^2 E\{r_I^2(t_2)\} + E\{n^2(t_1)n^2(t_2)\}dt_2 dt_1 \tag{D.19}$$

Using (D.10),

$$E\{C_4\} = \int_{\Gamma_j} \int_{\Gamma_l} E\{r_I^2(t_1)r_I^2(t_2)\}dt_2 dt_1 + \int_{\Gamma_j} \int_{\Gamma_l} E\{n^2(t_1)n^2(t_2)\}dt_2 dt_1 +$$

$$+ 2B\sigma^2 \left(|\Gamma_l| \int_{\Gamma_j} E\{r_I^2(t_1)\}dt_1 + |\Gamma_j| \int_{\Gamma_l} E\{r_I^2(t_2)\}dt_2 \right) +$$

$$+ \begin{cases} 4\sigma^2 \int\limits_{\Gamma_l} E\{r_I^2(t)\}dt & , j = l \\ 0 & , j \neq l \end{cases} \tag{D.20}$$

From (3.7) and (C.3),

$$\int_{\Gamma_j} \int_{\Gamma_l} E\{r_I^2(t_1)r_I^2(t_2)\}dt_2 dt_1 = \sum_{k_1,k_2,k_3,k_4} \frac{\sqrt{E_{k_1}E_{k_2}E_{k_3}E_{k_4}}}{4N_f^2} a_j^{(k_1)} a_j^{(k_2)} a_l^{(k_3)} a_l^{(k_4)} \tilde{g}$$

$$\times R_{\tilde{w}}^j((c_j^{(k_1)} - c_j^{(k_2)})T_c) R_{\tilde{w}}^l((c_l^{(k_3)} - c_l^{(k_4)})T_c) , \tag{D.21}$$

where

$$\tilde{g} = E\left\{\left(1 + b^{(k_1)}\tilde{d}_j^{(k_1)}\right)\left(1 + b^{(k_2)}\tilde{d}_j^{(k_2)}\right)\left(1 + b^{(k_3)}\tilde{d}_l^{(k_3)}\right)\left(1 + b^{(k_4)}\tilde{d}_l^{(k_4)}\right)\right\}$$

$$= \begin{cases} 4\left(1 + \tilde{d}_j^{(k_1)}\tilde{d}_l^{(k_2)}\right) & \text{if } k_1 = k_2 = k_3 = k_4 \\ 1 & \text{if } k_1 \neq k_2 \neq k_3 \neq k_4 \\ 4 & \text{if } (k_1 = k_2) \neq (k_3 = k_4) \\ 2\left(1 + \tilde{d}_j^{(k)}\tilde{d}_l^{(k)}\right) & \text{if three equal (k) one different} \\ \left(1 + \tilde{d}_j^{(k_1)}\tilde{d}_l^{(k_1)}\right)\left(1 + \tilde{d}_j^{(k_2)}\tilde{d}_l^{(k_2)}\right) & \text{if } (k_1 = k_3) \neq (k_2 = k_4) \\ & \text{or } (k_1 = k_4) \neq (k_2 = k_3) \end{cases}$$

(D.22)

The following equality can be obtained after some approximation [35, 28].

$$\int_{\Gamma_j}\int_{\Gamma_l} E\{n^2(t_1)n^2(t_2)\}dt_2dt_1 = 4B^2\sigma^4\left|\Gamma\right|^2\left(1 + \frac{1}{B|\Gamma|}\right).$$

(D.23)

Then, using the results above and assuming that $|\Gamma_j| = |\Gamma_l| = |\Gamma|$,

$$E\left\{C_4\right\} = 4B^2\sigma^4\left|\Gamma\right|^2\left(1 + \frac{1}{B|\Gamma|}\right) + \sum_{k_1,k_2,k_3,k_4}\frac{\sqrt{E_{k_1}E_{k_2}E_{k_3}E_{k_4}}}{4N_f^2}a_j^{(k_1)}a_j^{(k_2)}a_l^{(k_3)}a_l^{(k_4)}\tilde{g}$$

$$\times R_{\tilde{w}}^j((c_j^{(k_1)} - c_j^{(k_2)})T_c)R_{\tilde{w}}^l((c_l^{(k_3)} - c_l^{(k_4)})T_c)+$$

$$+ 2B\sigma^2\left|\Gamma\right|\sum_{k_1,k_2}\frac{\sqrt{E_{k_1}E_{k_2}}}{2N_f}(1 + \delta(k_1 - k_2))$$

$$\times \left[a_j^{(k_1)}a_j^{(k_2)}R_{\tilde{w}}^j((c_j^{(k_1)} - c_j^{(k_2)})T_c) + a_l^{(k_1)}a_l^{(k_2)}R_{\tilde{w}}^l((c_l^{(k_1)} - c_l^{(k_2)})T_c)\right]$$

$$+ 4\sigma^2\delta[j - l]\sum_{k_1,k_2}\frac{\sqrt{E_{k_1}E_{k_2}}}{2N_f}a_j^{(k_1)}a_j^{(k_2)}(1 + \delta(k_1 - k_2))R_{\tilde{w}}^j((c_j^{(k_1)} - c_j^{(k_2)})T_c)$$

(D.24)

The polarity randomization codes $a_j^{(2)}, \ldots, a_j^{(k)}$ can be assumed to be i.i.d. random variables that take values $\{-1, +1\}$ with equal probability. Then,

$$E\{C_1\} = \begin{cases} \sum\limits_{k=2}^{K} \frac{E_k}{N_f} \left[R_{\tilde{w}}^j ((c_j^{(1)} - c_j^{(k)}) T_c) \right]^2 + \sigma^2 \gamma_j^{(1)} & , \quad j = l \\ 0 & , \quad j \neq l \end{cases} \tag{D.25}$$

Also, it can be easily seen that

$$E\{C_2\} = E\{C_3\} = 0 . \tag{D.26}$$

$E\{C_4\}$:

Let $j \neq l$:

$$E\{C_4\} = 4B^2 \sigma^4 |\Gamma|^2 \left(1 + \frac{1}{B|\Gamma|} \right) + \sum_{k=2}^{K} \frac{E_k^2}{N_f^2} \left(1 + \tilde{d}_j^{(k)} \tilde{d}_l^{(k)} \right) (\chi_{j,k} \chi_{l,k})$$
$$+ \sum_{k_1 \neq k_2} \frac{E_{k_1} E_{k_2}}{N_f^2} \chi_{j,k_1} \chi_{l,k_2}$$
$$+ 2B\sigma^2 |\Gamma| \sum_{k=2}^{K} \frac{E_k}{N_f} (\chi_{j,k} + \chi_{l,k})$$

Let $j = l$: $\tag{D.27}$

$$E\{C_4\} = 4B^2 \sigma^4 |\Gamma|^2 \left(1 + \frac{1}{B|\Gamma|} \right) + 4\sigma^2 \sum_{k=2}^{K} \frac{E_k}{N_f} (B|\Gamma| + 1) \chi_{j,k}$$
$$+ \sum_{k=2}^{K} \frac{2E_k^2}{N_f^2} (\chi_{j,k})^2 + \sum_{k_1 \neq k_2} \frac{E_{k_1} E_{k_2}}{N_f^2} \chi_{j,k_1} \chi_{j,k_2} +$$
$$+ 2 \sum_{k_1 \neq k_2} \frac{E_{k_1} E_{k_2}}{N_f^2} \left[R_{\tilde{w}}^j ((c_j^{(k_1)} - c_j^{(k_2)}) T_c) \right]^2$$

$$\tag{D.28}$$

From (D.1),

$$E\{n_j n_l\} = \frac{2E_1}{N_f} a_j^{(1)} a_l^{(1)} E\{C_1\} + \sqrt{\frac{2E_1}{N_f}} a_j^{(1)} E\{C_2\} + \sqrt{\frac{2E_1}{N_f}} a_l^{(1)} E\{C_3\} + E\{C_4\}$$

$$\tag{D.29}$$

Finally, $E\{n_j n_l\}$ can be written as

$$
E\{n_j n_l\} =
\begin{cases}
\begin{aligned}
& 4B^2\sigma^4 |\Gamma|^2 \left(1 + \tfrac{1}{B|\Gamma|}\right) + \sum_{k=2}^{K} \tfrac{E_k^2}{N_f^2} \left(1 + \tilde{d}_j^{(k)} \tilde{d}_l^{(k)}\right) \chi_{j,k} \chi_{l,k} \\
& + 2B\sigma^2 |\Gamma| \sum_{k=2}^{K} \tfrac{E_k}{N_f} \left(\chi_{j,k} + \chi_{l,k}\right) \\
& + \sum_{k_1 \neq k_2} \tfrac{E_{k_1} E_{k_2}}{N_f^2} \chi_{j,k_1} \chi_{l,k_2} \ , \qquad\qquad\qquad\qquad\qquad j \neq l \\[2em]
& 4B^2\sigma^4 |\Gamma|^2 \left(1 + \tfrac{1}{B|\Gamma|}\right) + \sum_{k=2}^{K} \tfrac{2E_k^2}{N_f^2} \left(\chi_{j,k}\right)^2 + 4\sigma^2 \sum_{k=2}^{K} \tfrac{E_k}{N_f} \left(B|\Gamma| + 1\right) \chi_{j,k} \\
& + \sum_{k_1 \neq k_2} \tfrac{E_{k_1} E_{k_2}}{N_f^2} \left(\chi_{j,k_1} \chi_{j,k_2} + 2 \left[R_{\tilde{w}}^j ((c_j^{(k_1)} - c_j^{(k_2)}) T_c) \right]^2 \right) \\
& + \tfrac{2E_1}{N_f} \left[\sum_{k=2}^{K} \tfrac{E_k}{N_f} \left[R_{\tilde{w}}^j ((c_j^{(1)} - c_j^{(k)}) T_c) \right]^2 + \sigma^2 \gamma_j^{(1)} \right] , \qquad\qquad j = l
\end{aligned}
\end{cases}
$$

$$(\text{D.30})$$

APPENDIX E

Proof of Lemma 3.3

In Chapter 3, α_j is defined as

$$\alpha_j = \frac{E_1 \gamma_j^{(1)}}{N_f} \tilde{d}_j^{(1)} + \sqrt{\frac{2E_1}{N_f}} a_j^{(1)} \tilde{d}_j^{(1)} \int_{\Gamma_j} \tilde{w}(t - jT_f - c_j^{(1)} T_c)[r_I(t) + n(t)]dt \ . \quad \text{(E.1)}$$

Taking the expectation of both sides,

$$E\{\alpha_j\} = \frac{E_1 \gamma_j^{(1)}}{N_f} \tilde{d}_j^{(1)} + \sqrt{\frac{2E_1}{N_f}} a_j^{(1)} \tilde{d}_j^{(1)} \int_{\Gamma_j} \tilde{w}\left(t - jT_f - c_j^{(1)} T_c\right) E\{r_I(t)\} dt \ , \quad \text{(E.2)}$$

since $n(t)$ is zero mean Gaussian noise. From (3.6) and (3.7),

$$E\{\alpha_j\} = \frac{E_1 \gamma_j^{(1)}}{N_f} \tilde{d}_j^{(1)} + \sum_{k=2}^{K} \frac{\sqrt{E_1 E_k}}{N_f} a_j^{(1)} a_j^{(k)} \tilde{d}_j^{(1)} R_{\tilde{w}}^j((c_j^{(1)} - c_j^{(k)})T_c) \ . \quad \text{(E.3)}$$

The polarity randomization codes $a_j^{(2)}, \ldots, a_j^{(k)}$ can be assumed to be i.i.d. random variables that take values $\{-1, +1\}$ with equal probability. Then,

$$E\{\alpha_j\} = \frac{E_1}{N_f} \gamma_j^{(1)} \tilde{d}_j^{(1)} \ . \quad \text{(E.4)}$$

From (E.1) $\alpha_j \alpha_l$ can be written as

$$\alpha_j \alpha_l = \frac{E_1^2}{N_f^2} \gamma_j^{(1)} \gamma_l^{(1)} \tilde{d}_j^{(1)} \tilde{d}_l^{(1)} \tag{E.5}$$

$$+ \frac{E_1 \gamma_j^{(1)}}{N_f} \tilde{d}_j^{(1)} \sqrt{\frac{2E_1}{N_f}} a_l^{(1)} \tilde{d}_l^{(1)} \int_{\Gamma_l} \tilde{w}\left(t - lT_f - c_l^{(1)} T_c\right)\left(r_I(t) + n(t)\right)dt$$

$$+ \frac{E_1 \gamma_l^{(1)}}{N_f} \tilde{d}_l^{(1)} \sqrt{\frac{2E_1}{N_f}} a_j^{(1)} \tilde{d}_j^{(1)} \int_{\Gamma_j} \tilde{w}\left(t - jT_f - c_j^{(1)} T_c\right)\left(r_I(t) + n(t)\right)dt$$

$$+ \frac{2E_1}{N_f} a_j^{(1)} a_l^{(1)} \tilde{d}_j^{(1)} \tilde{d}_l^{(1)} C_1 \,,$$

where C_1 is given in (D.2).

Taking the expectation and using (3.6),

$$E\{\alpha_j \alpha_l\} = \frac{E_1^2 \gamma_j^{(1)} \gamma_l^{(1)}}{N_f^2} \tilde{d}_j^{(1)} \tilde{d}_l^{(1)} +$$

$$+ \frac{E_1 \gamma_j^{(1)}}{N_f} \tilde{d}_j^{(1)} a_l^{(1)} \tilde{d}_l^{(1)} \sum_{k=2}^{K} \frac{\sqrt{E_k E_1}}{N_f} a_l^{(k)} R_{\tilde{w}}^l((c_l^{(1)} - c_l^{(k)})T_c) +$$

$$+ \frac{E_1 \gamma_l^{(1)}}{N_f} \tilde{d}_l^{(1)} a_j^{(1)} \tilde{d}_j^{(1)} \sum_{k=2}^{K} \frac{\sqrt{E_k E_1}}{N_f} a_j^{(k)} R_{\tilde{w}}^j((c_j^{(1)} - c_j^{(k)})T_c) +$$

$$+ \frac{2E_1}{N_f} a_j^{(1)} a_l^{(1)} \tilde{d}_j^{(1)} \tilde{d}_l^{(1)} E\{C_1\} \tag{E.6}$$

The polarity randomization codes $a_j^{(2)}, \ldots, a_j^{(k)}$ can be assumed to be i.i.d. random variables that take values $\{-1, +1\}$ with equal probability. Then,

$$E\{\alpha_j \alpha_l\} = \begin{cases} \frac{E_1^2}{N_f^2} \gamma_j^{(1)} \gamma_l^{(1)} \tilde{d}_j^{(1)} \tilde{d}_l^{(1)} & , j \neq l \\[4mm] \frac{E_1^2}{N_f^2}(\chi_{j,1})^2 + \frac{2E_1}{N_f}\left[\sum_{k=2}^{K} \frac{E_k}{N_f}\left[R_{\tilde{w}}^j((c_j^{(1)} - c_j^{(k)})T_c)\right]^2 + \sigma^2 \gamma_j^{(1)}\right] & , j = l \end{cases} \tag{E.7}$$

Bibliography

[1] S. Gezici, "Coded-reference ultra-wideband systems," in *Proc. IEEE International Conference on Ultra-Wideband*, vol. 3, pp. 117–120, Sept. 2008.

[2] S. Gezici, H. Kobayashi, H. V. Poor, and A. F. Molisch, "Performance evaluation of impulse radio UWB systems with pulse-based polarity randomization," *IEEE Transactions on Signal Processing*, vol. 53, pp. 2537–2549, July 2005.

[3] H. Arslan, Z. N. Chen, and M.-G. D. Benedetto, eds., *Ultra Wideband Wireless Communications Systems*. Hoboken: Wiley-Interscience, 2006.

[4] Z. Sahinoglu, S. Gezici, and I. Guvenc, *Ultra-Wideband Positioning Systems: Theoretical Limits, Ranging Algorithms, and Protocols*. Cambridge University Press, 2008.

[5] S. Gezici, Z. Tian, G. B. Giannakis, H. Kobayashi, A. F. Molisch, H. V. Poor, and Z. Sahinoglu, "Localization via ultra-wideband radios: A look at positioning aspects for future sensor networks," *IEEE Signal Processing Magazine*, vol. 22, pp. 70–84, July 2005.

[6] M. Z. Win and R. A. Scholtz, "Impulse radio: How it works," *IEEE Communications Letters*, vol. 2, pp. 36–38, Feb. 1998.

[7] M. Z. Win, R. A. Scholtz, and L. W. Fullerton, "Time-hopping SSMA techniques for impulse radio with an analog modulated data subcarrier," in

Proc. IEEE 4th International Symposium on Spread Spectrum Techniques and Applications, vol. 1, pp. 359–364, Sept. 1996.

[8] D. Cassioli, M. Z. Win, and A. F. Molisch, "The ultra-wide bandwidth indoor channel: from statistical model to simulations," *IEEE Journal on Selected Areas in Communications*, vol. 20, pp. 1247–1257, Aug. 2002.

[9] H. Zhang and D. L. Goeckel, "Generalized transmitted-reference UWB systems," in *Proc. IEEE Conference on Ultra Wideband Systems and Technologies*, pp. 147–151, Nov. 2003.

[10] M. Z. Win and R. A. Scholtz, "Ultra-wide bandwidth time-hopping spread-spectrum impulse radio for wireless multiple-access communications," *IEEE Transactions on Communications*, vol. 48, pp. 679–689, Apr. 2000.

[11] S. Gezici and Z. Sahinoglu, "Theoretical limits for estimation of vital signal parameters using impulse radio uwb," in *Proc. IEEE International Conference on Communications*, pp. 5751–5756, June 2007.

[12] Y.-P. Nakache and A. F. Molisch, "Spectral shape of uwb signals - influence of modulation format, multiple access scheme and pulse shape," *IEEE Vehicular Technology Conference*, vol. 4, pp. 2510–2514, Apr. 2003.

[13] S. Gezici, M. Chiang, H. V. Poor, and H. Kobayashi, "Optimal and suboptimal finger selection algorithms for mmse rake receivers in impulse radio ultra-wideband systems," in *IEEE Wireless Communications and Networking Conference*, vol. 2, pp. 861–866, March 2005.

[14] M. Z. Win and R. A. Scholtz, "On the energy capture of ultrawide bandwidth signals in dense multipath environments," *IEEE Communications Letters*, vol. 2, pp. 245–247, Sept. 1998.

[15] R. J.-M. Cramer, R. A. Scholtz, and M. Z. Win, "Evaluation of an ultra-wide-band propagation channel," *IEEE Transactions on Antennas and Propagation*, vol. 50, pp. 561–570, May 2002.

[16] R. Hoctor and H. Tomlinson, "Delay-hopped transmitted-reference rf communications," in *IEEE Conference on Ultra Wideband Systems and Technologies*, pp. 265–269, May 2002.

[17] J. D. Choi and W. E. Stark, "Performance of ultra-wideband communications with suboptimal receivers in multipath channels," *IEEE Journal on Selected Areas in Communications*, vol. 20, pp. 1754–1766, Dec. 2002.

[18] Y.-L. Chao, "Optimal integration time for uwb transmitted reference correlation receivers," in *Conference Record of the Thirty-Eighth Asilomar Conference on Signals, Systems and Computers*, vol. 1, pp. 647–651, Nov. 2004.

[19] N. van Stralen, A. Dentinger, K. W. II, R. G. Jr., R. Hoctor, and H. Tomlinson, "Delay hopped transmitted reference experimental results," in *Proc. IEEE Conference on Ultra Wideband Systems and Technologies*, pp. 93–98, May 2002.

[20] D. L. Goeckel and Q. Zhang, "Slightly frequency-shifted reference ultra-wideband (uwb) radio," *IEEE Transactions on Communications*, vol. 55, pp. 508–519, March 2007.

[21] J. Zhang, H.-Y. Hu, L.-K. Liu, and T.-F. Li, "Code-orthogonalized transmitted-reference ultra-wideband (uwb) wireless communication system," in *International Conference on Wireless Communications, Networking and Mobile Computing*, (Shanghai), pp. 528–532, Sept. 2007.

[22] A. A. D'amico and U. Mengali, "Code-multiplexed uwb transmitted-reference radio," *IEEE Transactions on Communications*, vol. 56, pp. 2125–2132, Dec. 2008.

[23] E. Fishler and H. V. Poor, "Low-complexity multiuser detectors for time-hopping impulse-radio systems," *IEEE Transactions on Signal Processing*, vol. 52, pp. 2561–2571, Sept. 2004.

[24] S. Gezici, H. Kobayashi, and H. V. Poor, "A comparative study of pulse combining schemes for impulse radio uwb systems," in *Proc. IEEE Sarnoff Symposium on Advances in Wired and Wireless Communication*, pp. 7–10, Apr. 2004.

[25] P. A. Humblet and M. Azizoğlu, "On the bit error rate of lightwave systems with optical amplifiers," *Journal of Lightwave Technology*, vol. 9, pp. 1576 – 1582, Nov. 1991.

[26] G. N. Georgiev and M. N. Georgieva-Grosse, "Methods for evaluation of the Euler gamma function in the complex field and their application in the computational electromagnetics," in *Proc. International Conference on Transparent Optical Networks (ICTON)*, (Germany), pp. 1–5, June 2010.

[27] M. Abramowitz and I. A. Stegun, eds., *Handbook of Mathematical Functions: with Formulas, Graphs, and Mathematical Tables.* New York: Dover, 1965.

[28] A. A. D'amico and U. Mengali, "Code-multiplexed transmitted-reference UWB systems in a multi-user environment," *IEEE Transactions on Communications*, vol. 58, pp. 966–974, March 2010.

[29] A. F. Molisch, K. Balakrishnan, C.-C. Chong, S. Emami, A. Fort, J. Karedal, J. Kunisch, H. Schantz, U. Schuster, and K. Siwiak, "802.15.4a channel model - final report," tech. rep., IEEE, 2005.

[30] S. Verdu, *Multiuser Detection.* 1st ed. Cambridge, UK: Cambridge University Press, 1998.

[31] H. V. Poor, *An Introduction to Signal Detection and Estimation.* New York: Springer-Verlag, 1994.

[32] F. Ramirez-Mireles and R. A. Scholtz, "Multiple-access performance limits with time hopping and pulse position modulation," in *Proc. IEEE Military Communications Conference*, vol. 2, pp. 529–533, Oct. 1998.

[33] J. G. Proakis, *Digital Communications*. New York: McGraw-Hill, 4 ed., 2001.

[34] Z. Tian and B. M. Sadler, "Weighted energy detection of ultra-wideband signals," in *Proc. IEEE 6th Workshop on Signal Processing Advances in Wireless Communications*, pp. 1068–1072, June 2005.

[35] A. Papoulis, *Probability, Random Variables and Stochastic Processes*. New York: McGraw-Hill, 3 ed., 1991.